Extensive Test and Evaluation of CHARMM36IDPSFF Force Field for Intrinsically Disordered Protein and Folded Protein

Hao Liu[1], Dong Song[1], Yangpeng Zhang[1], Sheng Yang[1], Ray Luo[2,*], and Hai-Feng Chen[1,3,*]

[1]State Key Laboratory of Microbial Metabolism, Department of Bioinformatics and Biostatistics, SJTU-Yale Joint Center for Biostatistics, National Experimental Teaching Center for Life Sciences and Biotechnology, School of Life Sciences and Biotechnology, Shanghai Jiao Tong University, 800 Dongchuan Road, Shanghai, 200240, China
[2]Departments of Molecular Biology and Biochemistry, Chemical Engineering and Materials Science, Biomedical Engineering, University of California, Irvine, California 92697-3900, USA
[3]Shanghai Center for Bioinformation Technology, 1278 Keyuan Road, Shanghai, 200235, China

*Corresponding authors
Email addresses: haifengchen@sjtu.edu.cn; rluo@uci.edu;
Tel: 86-21-34204348
Fax: 86-21-34204348

The authors declare that there is no conflict of interest.

Table S1. Karplus equations used to calculate the scalar couplings.

Scalar couplings	Karplus equations
$^3J_{HNH\alpha}$[1]	$_3J_i = 8.40\cos^2(\varphi_i - 60°) - 1.36\cos(\varphi_i - 60°) + 0.33$
$^3J_{HNC\beta}$[1]	$_3J_i = 3.71\cos^2(\varphi_i + 60°) - 0.59\cos(\varphi_i + 60°) + 0.08$
$^3J_{HNC}$[1]	$_3J_i = 4.36\cos^2(\varphi_i + 180°) - 1.08\cos(\varphi_i + 180°) + 0.01$
$^3J_{H\alpha C}$[2]	$_3J_i = 3.72\cos^2(\varphi_i + 120°) - 2.18\cos(\varphi_i + 120°) + 1.28$
$^3J_{HNC\alpha}$[3]	$_3J_i$ $= -0.23\cos(\varphi_i) - 0.20\cos(\psi_{i-1}) + 0.07\sin(\varphi_i) + 0.08\sin$
$^3J_{CC}$[4]	$_3J_i = 1.78\cos^2(\varphi_i) - 0.95\cos(\varphi_i) + 0.46$
$^2J_{NC\alpha}$[5]	$_2J_i = -0.66\cos^2(\psi_{i-1}) + 1.52\cos(\psi_{i-1}) + 7.85$
$^1J_{NC\alpha}$[6]	$_1J_i = 1.70\cos^2(\psi_i) - 0.98\cos(\psi_i) + 9.51$
$^1J_{H\alpha C\alpha}$[7]	$_1J_i = 1.4\sin(\psi_i + 138°) - 4.1\cos(2(\psi_i + 138°)) + 1.7\cos(2(\varphi_i + 30)) + R_a$

[a]. R is a residue-specific value.

$R =$ 143.9 for ALA, 142.8 for ARG, 144.5 for ASN, 144.4 for ASP,

143.5 for CYS, 142.9 for GLN, 142.8 for GLU, 143.9 for HIS,

141.7 for ILE, 142.5 for LEU, 142.8 for LYS, 142.8 for MET,

144.0 for PHE, 150.1 for PRO, 143.5 for SER, 142.4 for THR,

144.1 for TRP, 144.1 for TYR, 141.7 for VAL.

Table S2. RMS errors between the simulation and experimental chemical shifts for all tested peptides and proteins. All the units are in ppm.

System	Force filed & water model	Cα	Cβ	C	N	Hα	HN
ALA$_5$	C36IDPSFF	0.16	0.20	0.34	0.63	0.02	0.33
ALA$_7$	C36IDPSFF	0.09	0.20	0.30	0.63	0.02	0.28
Aβ40 (PDB)	C36IDPSFF	0.39	0.40		1.96	0.12	0.31
Aβ40 (PDB)	C36IDPSFF/disp-water	0.38	0.33		1.43	0.10	0.31
Aβ40 (Extended)	C36IDPSFF	0.37	0.38		1.67	0.12	0.27
Aβ42	C36IDPSFF	0.44	0.48		1.76	0.21	0.22
ACTR	C36IDPSFF	0.69	0.33	0.57	1.38		0.17
ACTR	C36IDPSFF/disp-water	0.52	0.26	0.55	1.11		0.15
drkN SH3	C36IDPSFF	0.52	0.46	0.95	1.27		0.19
drkN SH3	C36IDPSFF/disp-water	0.72	0.44	1.11	1.07		0.22
hIAPP	C36IDPSFF	0.71	0.49		1.95	0.12	0.28
Histatin-5	C36IDPSFF					0.06	0.26
Trp-cage	C36IDPSFF					0.31	0.36
BPTI	C36IDPSFF	0.77	1.58	0.66	1.57	0.18	0.33
GB3	C36IDPSFF	1.18	0.75	0.66	1.65	0.18	0.29
HEWL	C36IDPSFF	0.75	1.66	1.13	1.48		
2JPU	C36IDPSFF	1.04	0.62	0.66	1.34	0.13	0.33
2JQN	C36IDPSFF	0.91	0.81	0.77	1.62	0.17	0.42
2KL6	C36IDPSFF	1.06	1.42	1.01	3.54	0.31	0.59

Table S3. RMS errors between the experimental scalar couplings and simulate values of C36IDPSFF for the tested peptides and proteins. All the units are in Hz.

Systems	Scalar Couplings	RMS error	
		C36IDPSFF	C36IDPSFF/disp-water
ALA$_5$	$^3J_{HNH\alpha}$	0.08	
	$^3J_{HNC\beta}$	0.17	
	$^3J_{H\alpha C}$	0.04	
	$^3J_{HNC}$	0.06	
	$^3J_{HNC\alpha}$	0.09	
	$^2J_{NC\alpha}$	0.42	
	$^1J_{NC\alpha}$	0.23	
ALA$_7$	$^3J_{HNH\alpha}$	0.08	
	$^3J_{HNC\beta}$	0.17	
	$^3J_{H\alpha C}$	0.19	
	$^3J_{HNC}$	0.12	
	$^3J_{HNC\alpha}$	0.09	
	$^2J_{NC\alpha}$	0.32	
	$^1J_{NC\alpha}$	0.26	
Aβ40 (PDB)	$^3J_{HNH\alpha}$	0.57	0.42
	$^3J_{H\alpha C}$	0.43	0.43
	$^3J_{CC}$	0.18	0.17
	$^2J_{NC\alpha}$	0.74	0.50
	$^1J_{NC\alpha}$	0.37	0.37
	$^1J_{H\alpha C\alpha}$	1.47	1.37
Aβ40 (Extended)	$^3J_{HNH\alpha}$	0.56	
	$^3J_{H\alpha C}$	0.33	
	$^3J_{CC}$	0.18	
	$^2J_{NC\alpha}$	0.55	
	$^1J_{NC\alpha}$	0.36	
	$^1J_{H\alpha C\alpha}$	1.48	
Aβ42		0.68	
drkN SH3	$^3J_{HNH\alpha}$	1.22	
Histatin-5		0.84	
BPTI		0.94	
GB3	$^3J_{HNH\alpha}$	1.10	
	$^3J_{HNC\beta}$	0.47	
	$^3J_{HNC}$	0.59	

Table S4. Comparison of experimental data and Cα calculated chemical shifts in simulations of Aβ40 started from PDB structure and extended structure. Experimental data were taken from Ref[8]. Standard errors of the mean are provided using block analysis. All units are in ppm.

| Residues | Initial Structure | | Exp. | Residues | Initial Structure | | Exp. |
	PDB	Extended			PDB	Extended	
A2	-0.34 ± 0.03	-0.29 ± 0.00	0.31	A21	-0.33 ± 0.00	-0.31 ± 0.02	0.01
E3	0.70 ± 0.01	0.49 ± 0.00	-0.21	E22	0.30 ± 0.00	-0.02 ± 0.03	-0.31
F4	-0.17 ± 0.01	-0.09 ± 0.02	-0.17	D23	-0.37 ± 0.02	-0.29 ± 0.02	-0.23
R5	-0.55 ± 0.01	-0.43 ± 0.01	-0.38	V24	0.42 ± 0.03	0.46 ± 0.02	0.66
H6	1.24 ± 0.00	0.97 ± 0.00	1.28	G25	0.28 ± 0.03	0.40 ± 0.04	0.30
D7	-0.01 ± 0.01	-0.10 ± 0.01	-0.24	S26	-0.21 ± 0.05	-0.14 ± 0.02	0.17
S8	0.24 ± 0.01	0.14 ± 0.01	0.63	N27	0.13 ± 0.04	0.08 ± 0.00	0.29
G9	0.12 ± 0.02	0.11 ± 0.01	0.22	K28	-0.25 ± 0.01	0.00 ± 0.01	0.37
Y10	-0.07 ± 0.05	-0.43 ± 0.03	0.25	G29	0.03 ± 0.00	0.03 ± 0.02	-0.01
E11	-0.11 ± 0.03	-0.42 ± 0.00	-0.22	A30	-0.34 ± 0.01	-0.26 ± 0.00	0.06
V12	0.20 ± 0.06	-0.36 ± 0.00	0.60	I31	-0.13 ± 0.00	-0.16 ± 0.03	-0.09
H13	1.12 ± 0.03	1.07 ± 0.03	0.79	I32	0.71 ± 0.02	-0.02 ± 0.01	-0.08
H14	1.71 ± 0.02	1.01 ± 0.04	1.03	G33	0.33 ± 0.01	0.04 ± 0.01	-0.01
Q15	0.04 ± 0.01	-0.55 ± 0.02	0.50	L34	-0.23 ± 0.01	-0.03 ± 0.04	0.07
K16	0.31 ± 0.03	-0.14 ± 0.02	0.15	M35	-0.25 ± 0.00	-0.28 ± 0.03	0.14
L17	0.11 ± 0.02	-0.34 ± 0.02	-0.06	V36	-0.27 ± 0.05	-0.09 ± 0.02	0.31
V18	-0.27 ± 0.05	-0.23 ± 0.13	-0.33	G37	0.33 ± 0.02	0.25 ± 0.01	0.06
F19	-0.10 ± 0.01	-0.29 ± 0.03	-0.39	G38	0.13 ± 0.01	0.09 ± 0.02	-0.10
F20	-0.56 ± 0.01	-0.51 ± 0.00	-0.47	V39	-0.37 ± 0.02	-0.15 ± 0.03	0.12
RMS error	0.39	0.37					

Table S5. Comparison of experimental data and calculated $^3J_{HNH\alpha}$ scalar couplings in simulations of Aβ40 started from PDB structure and extended structure. Experimental data were taken from Ref[9]. Standard errors of the mean are provided using block analysis. All units are in Hz.

Residues	Initial Structure		Exp.	Residues	Initial Structure		Exp.
	PDB	Extended			PDB	Extended	
A2	5.94 ± 0.14	6.04 ± 0.07	-	A21	6.29 ± 0.05	6.05 ± 0.09	5.60
E3	6.80 ± 0.02	7.01 ± 0.09	6.30	E22	7.00 ± 0.14	6.59 ± 0.16	5.95
F4	6.88 ± 0.09	7.18 ± 0.11	7.02	D23	7.30 ± 0.11	7.21 ± 0.09	6.64
R5	6.74 ± 0.17	7.24 ± 0.10	7.25	V24	6.41 ± 0.25	6.59 ± 0.11	6.82
H6	6.03 ± 0.18	6.95 ± 0.11	-	G25	5.92 ± 0.16	5.90 ± 0.11	5.96
D7	7.06 ± 0.12	7.25 ± 0.12	6.86	S26	6.72 ± 0.14	7.03 ± 0.15	6.51
S8	6.52 ± 0.19	6.76 ± 0.10	5.86	N27	7.26 ± 0.18	7.38 ± 0.11	7.32
G9	5.81 ± 0.14	5.69 ± 0.09	6.35	K28	7.63 ± 0.09	7.17 ± 0.08	6.46
Y10	6.99 ± 0.05	7.19 ± 0.15	6.38	G29	6.25 ± 0.18	5.80 ± 0.16	6.03
E11	7.25 ± 0.13	7.29 ± 0.08	6.29	A30	5.66 ± 0.19	5.88 ± 0.14	5.49
V12	7.07 ± 0.17	8.04 ± 0.13	6.78	I31	7.34 ± 0.11	7.60 ± 0.11	7.65
H13	6.71 ± 0.23	7.18 ± 0.15	7.25	I32	6.13 ± 0.07	7.79 ± 0.09	7.45
H14	6.99 ± 0.12	7.16 ± 0.13	-	G33	5.35 ± 0.13	5.66 ± 0.17	5.96
Q15	6.95 ± 0.10	7.55 ± 0.09	6.26	L34	7.25 ± 0.16	7.19 ± 0.18	6.72
K16	6.77 ± 0.11	7.34 ± 0.18	6.22	M35	7.28 ± 0.08	7.17 ± 0.17	7.25
L17	7.51 ± 0.23	7.22 ± 0.10	6.69	V36	7.18 ± 0.15	7.15 ± 0.09	7.49
V18	7.85 ± 0.15	8.04 ± 0.15	8.30	G37	5.86 ± 0.09	6.10 ± 0.09	5.98
F19	8.05 ± 0.13	7.86 ± 0.09	7.70	G38	5.88 ± 0.04	6.00 ± 0.08	5.99
F20	7.65 ± 0.16	7.86 ± 0.10	7.74	V39	7.55 ± 0.11	7.86 ± 0.09	7.94
RMS error	0.57	0.56					

Table S6. Difference between experimental data and simulated observables from C36IDPSFF in this study and a99SB-disp in previous work. The differences of chemical shifts and J-couplings were estimated by RMS errors, and the differences of RDCs were estimated by Q factors. The differences of Rg were estimated by $Rg_{Penalty}$ same with previous work. The $^3J_{HNH\alpha}$ couplings were compared and refered to ^3J here.

Proteins	Force Field & water model	Differences between Exp. and Sim.								
		Cα	Cβ	C	N	Hα	HN	^3J	RDCs	Rg
AB40	a99SB-disp	0.47	0.40		1.54	0.09	0.29	0.64	0.50	0.05
	C36IDPSFF	0.42	0.76		1.31	0.14	0.24	0.57	0.77	0.07
ACTR	a99SB-disp	0.46	0.30	0.42	0.87		0.18		0.81	0.11
	C36IDPSFF	0.69	0.57	0.60	1.22		0.17		0.93	0.44
drkN SH3	a99SB-disp	0.50	0.50	0.65		0.10	0.23	0.70	0.91	0.08
	C36IDPSFF	0.54	0.66	0.62		0.14	0.22	1.22	0.70	0.13
2JPU	a99SB-disp	1.205	0.814	0.951	1.976	0.179	0.376			
	C36IDPSFF	1.39	0.91	1.05	2.32	0.43	0.25			
2JQN	a99SB-disp	1.458	1.418	1.333	2.924	0.315	0.572			
	C36IDPSFF	1.33	1.27	1.29	2.66	0.29	0.51			
2KL6	a99SB-disp	1.033	1.145	0.998	3.028	0.275	0.561			
	C36IDPSFF	1.10	1.44	0.93	2.08	0.38	0.30			
BPTI	a99SB-disp							1.22		
	C36IDPSFF							0.94		
GB3	a99SB-disp							1.13[a]		
	C36IDPSFF							0.77[a]		

[a]. The $^3J_{HNH\alpha}$, $^3J_{HNC\beta}$, and $^3J_{HNC}$ of GB3 are all considered as ^3J here.
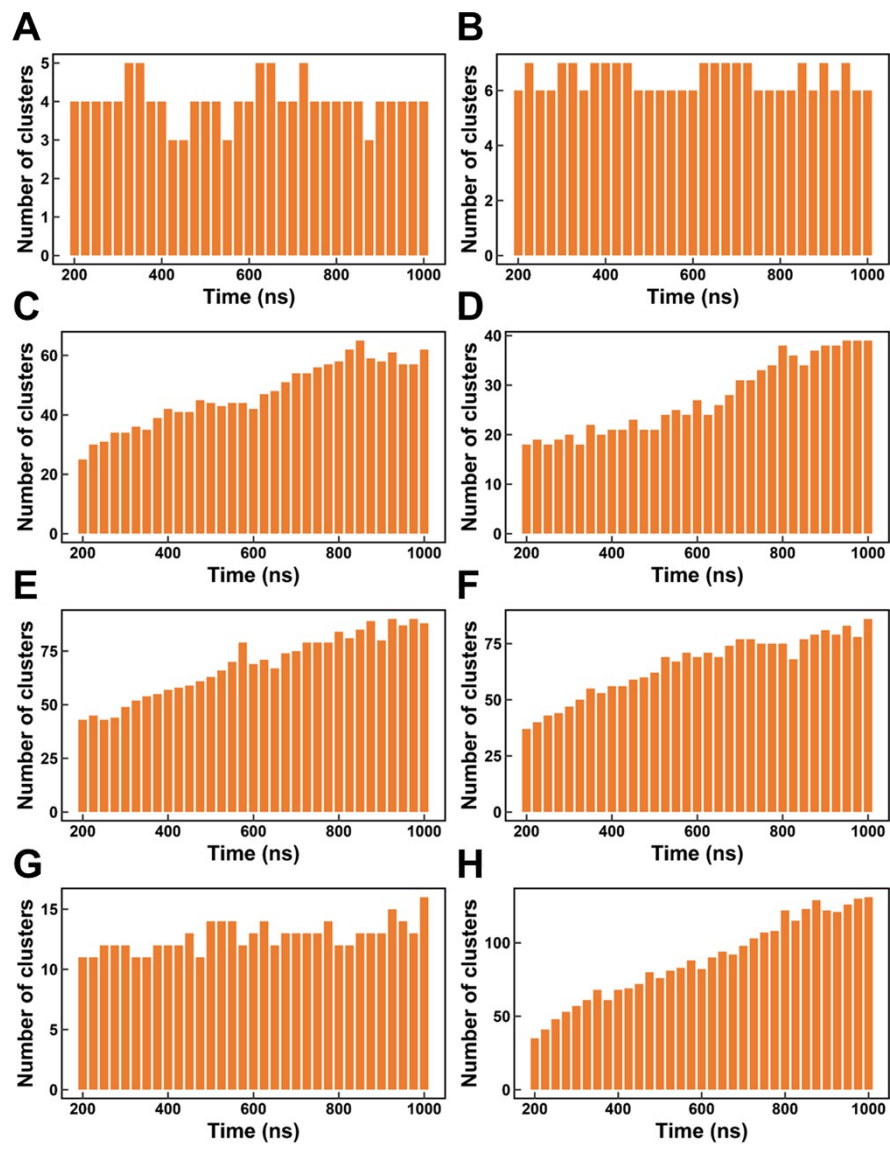
Fig. S1. Time-dependent number of conformation clusters for disordered peptides and protiens. (a) ALA$_5$. (b) ALA$_7$. (c) Aβ40. (d) Aβ42. (e) ACTR. (f) drkN SH3 (g) hIAPP. (h) Histatin-5.
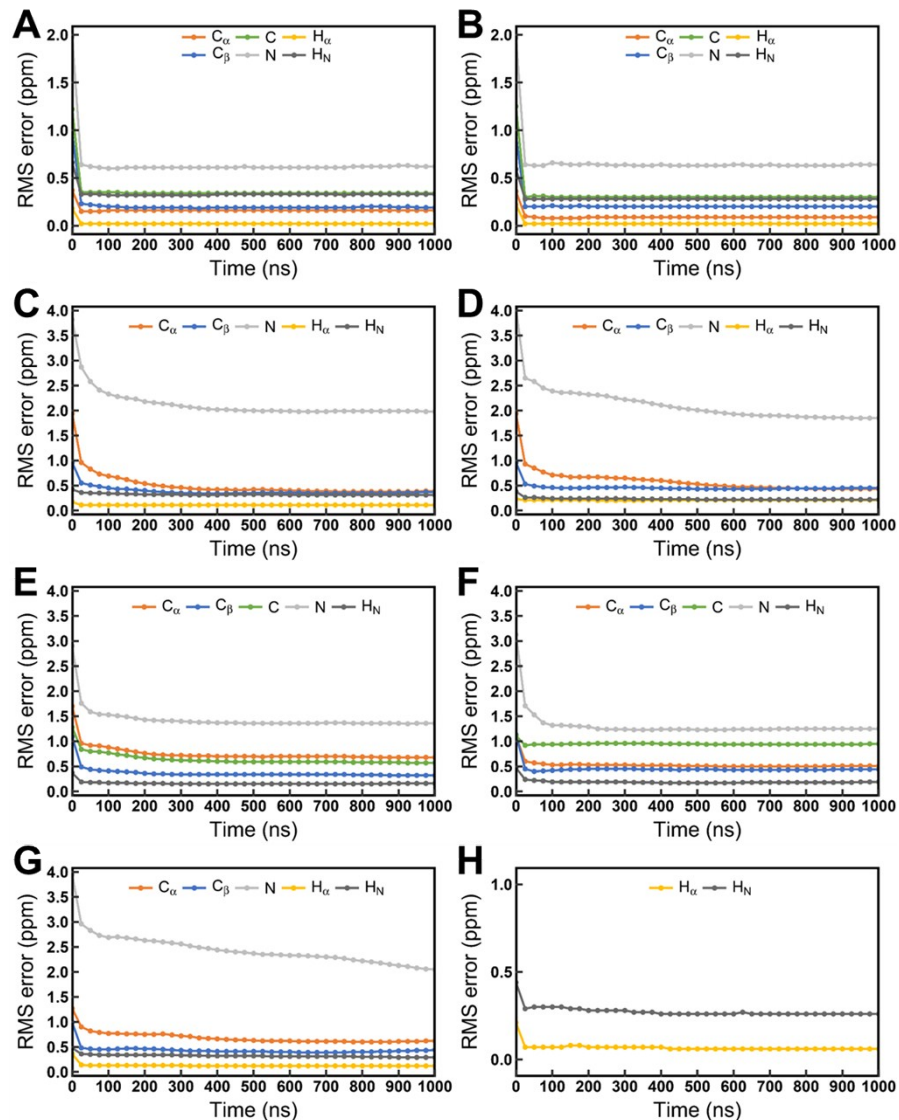
Fig. S2. Time-dependent RMS errors between experimental data and cumulative-averaged simulated chemical shifts for disordered peptides and proteins. (a) ALA5. (b) ALA7. (c) Aβ40. (d) Aβ42. (e) ACTR. (f) drkN SH3 (g) hIAPP. (h) Histatin-5.
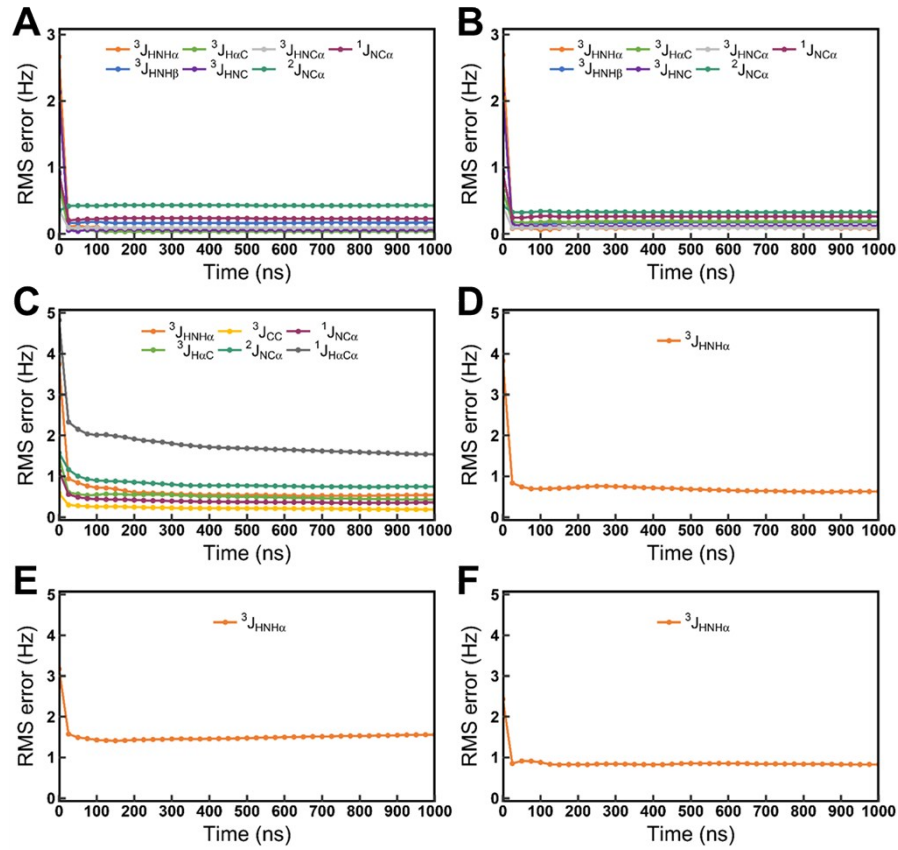
Fig. S3. Time-dependent RMS errors between experimental data and cumulative-averaged simulated scalar couplings for disordered peptides and proteins. (a) ALA5. (b) ALA7. (c) Aβ40. (d) Aβ42. (e) drkN SH3. (f) Histatin-5.
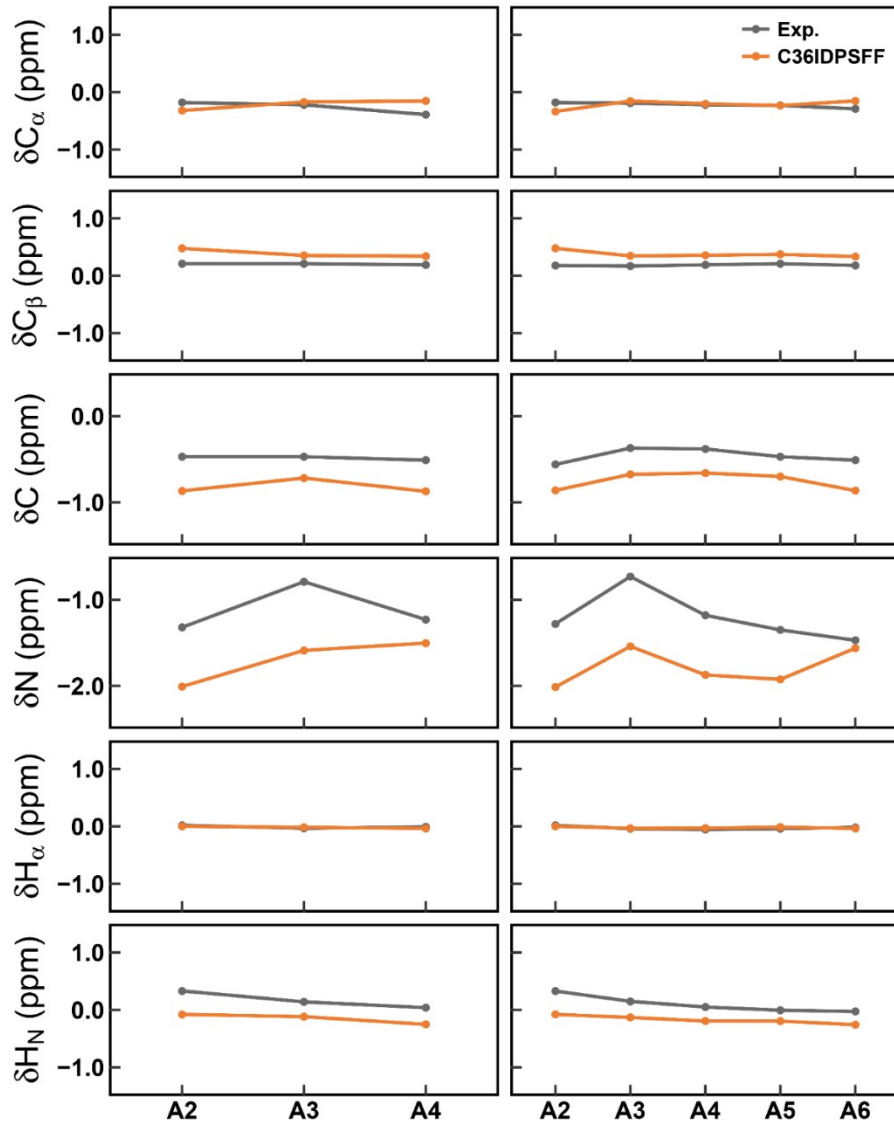
Fig. S4. Comparison of Simulated and experimental chemical shifts of Cα, Cβ, C, N, Hα, and HN atoms for ALA$_5$ and ALA$_7$. The left panel stands for ALA$_5$ and the right panel stands for ALA$_7$. Experimental values were taken from Ref[10].
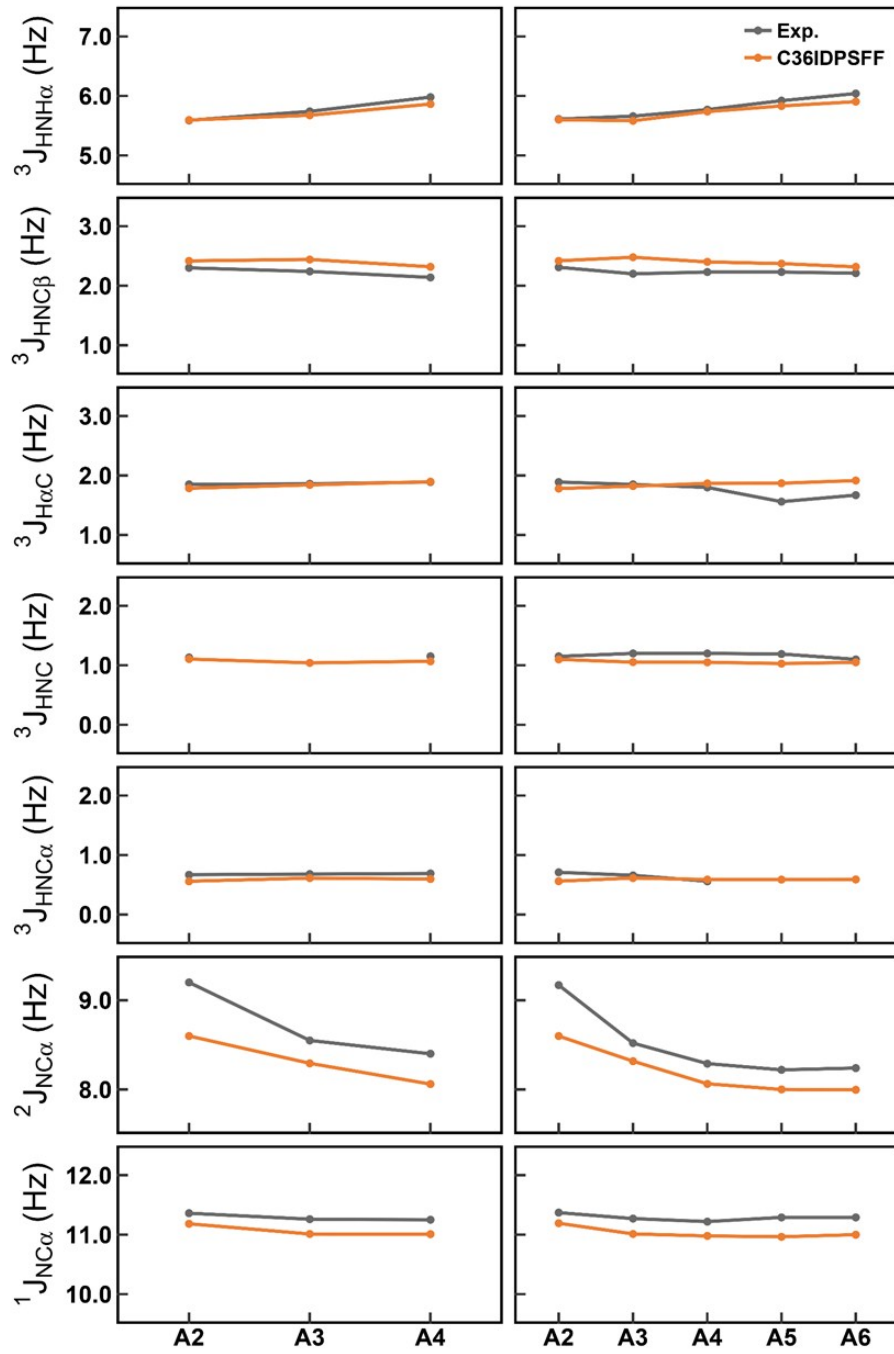
Fig. S5. Comparison of Simulated and experimental backbone scalar couplings $^3J_{HNH\alpha}$, $^3J_{HNC\beta}$, $^3J_{H\alpha C}$, $^3J_{HNC}$, $^3J_{HNC\alpha}$, $^2J_{NC\alpha}$, and $^1J_{NC\alpha}$ for ALA$_5$ and ALA$_7$. The left panel stands for ALA$_5$ and the right panel stands for ALA$_7$. Experimental values were taken from Ref[10].
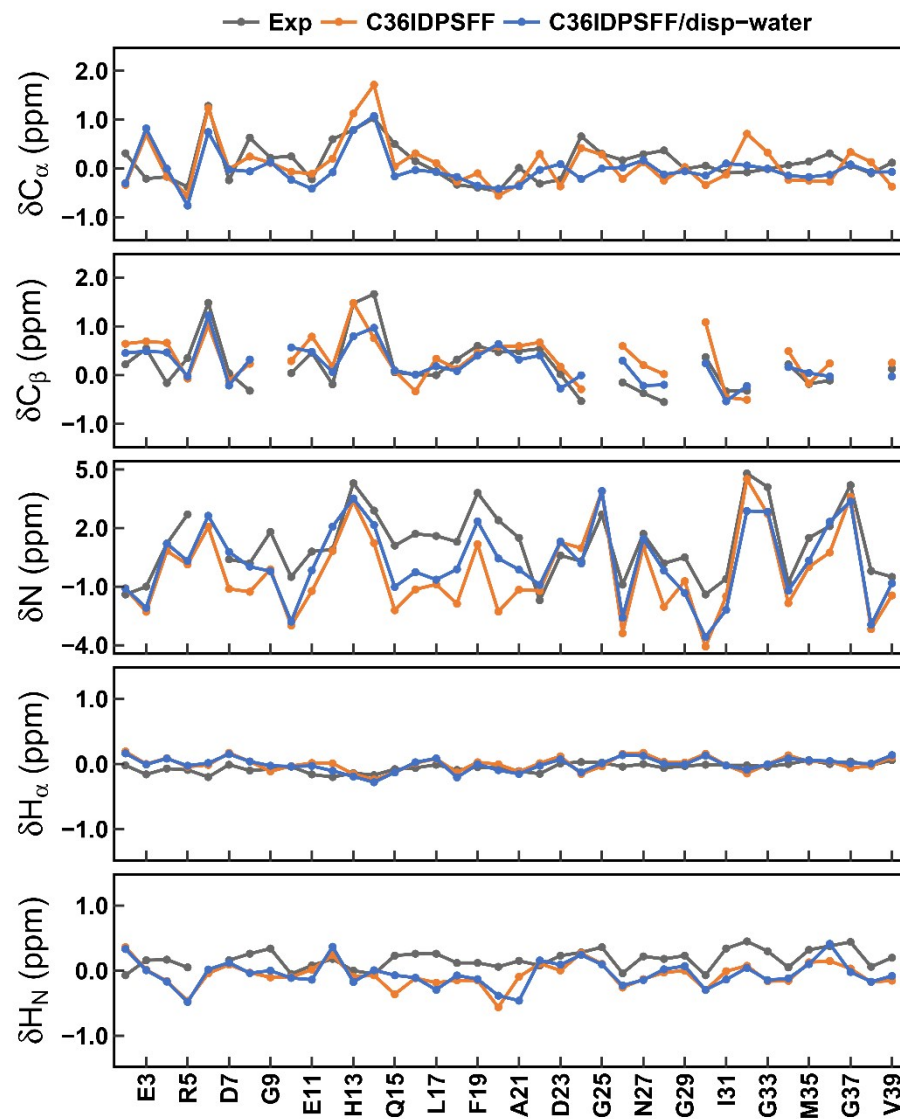
Fig. S6. Comparison of Simulated and experimental chemical shifts of Cα, Cβ, N, Hα, and HN atoms for AB40. The initial structures of MD simulations are retrieved from the PDB structure with the last two residues removed. Experimental values were taken from Ref[8].
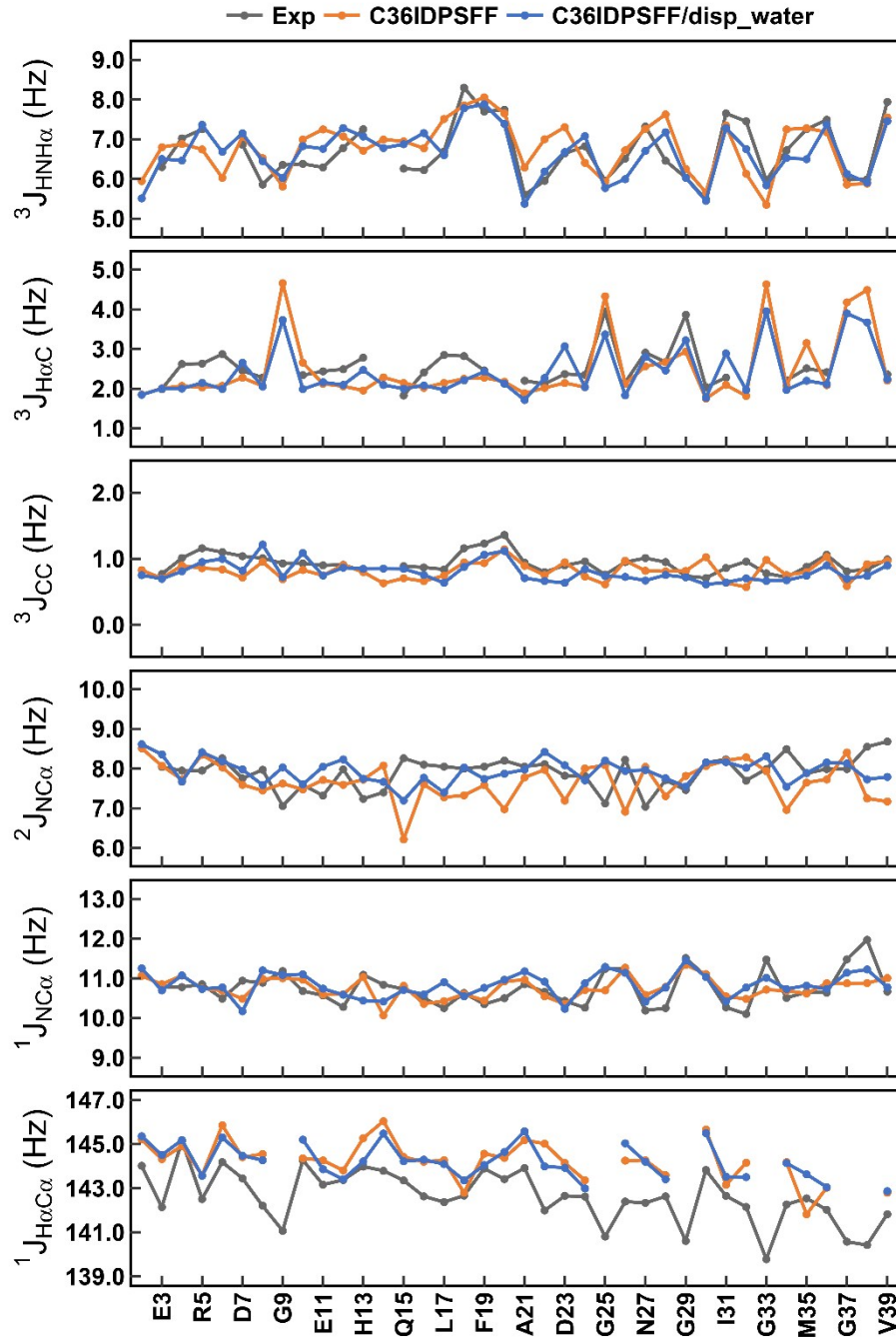
Fig. S7. Comparison of Simulated and experimental backbone scalar couplings $^3J_{HNH\alpha}$, $^3J_{H\alpha C}$, $^3J_{CC}$, $^2J_{NC\alpha}$, $^1J_{NC\alpha}$, and $^1J_{H\alpha C\alpha}$ for Aβ40. The initial structures of MD simulations are retrieved from the PDB structure with the last two residues removed. Experimental values were taken from Ref[9].
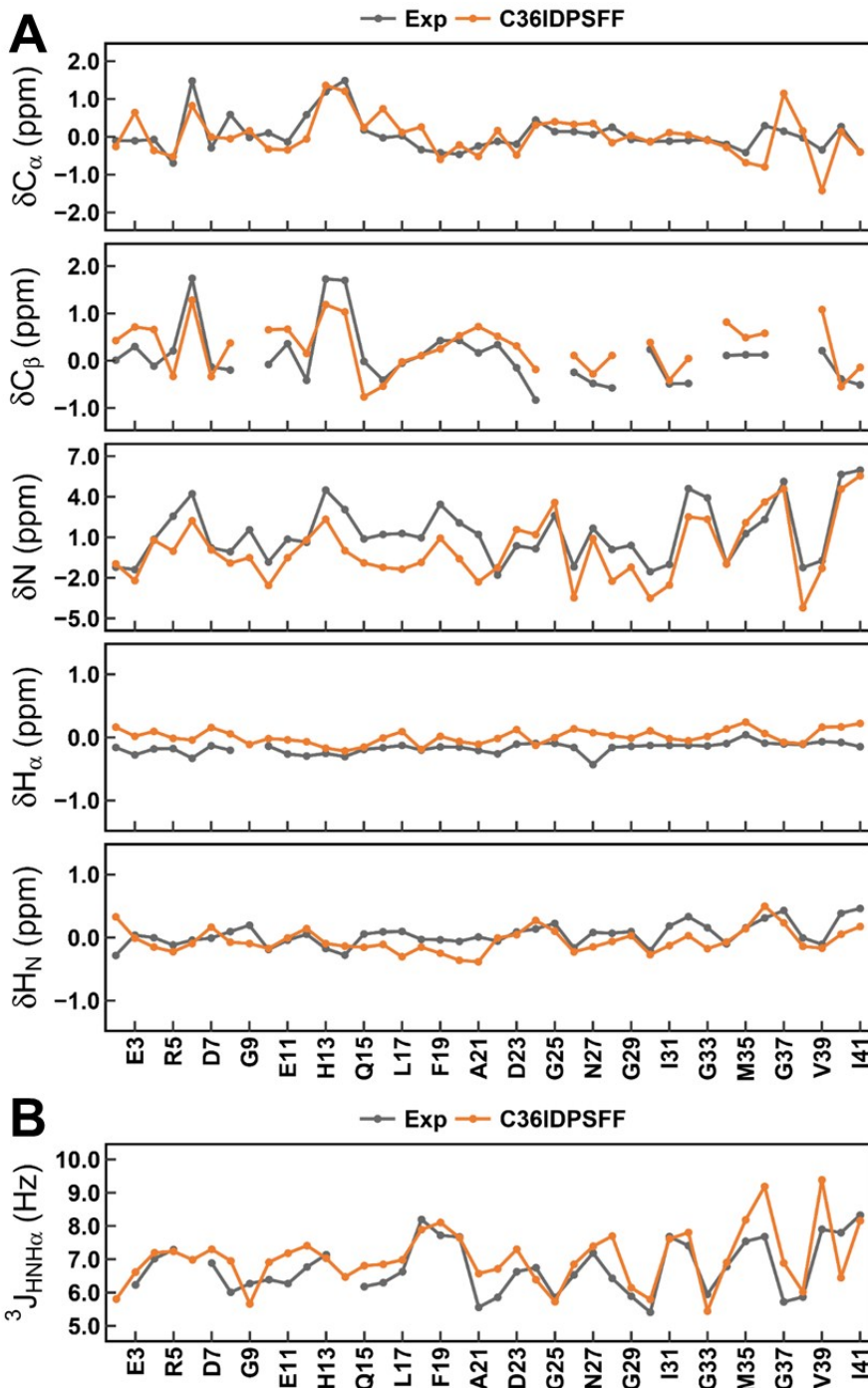
Fig. S8. Comparison of Simulated and experimental NMR observables for Aβ42. (a) Chemical shifts of Cα, Cβ, N, Hα, and HN atoms. (b) Backbone scalar couplings $^3J_{HNH\alpha}$. Experimental chemical shifts values were taken from Ref[11] and experimental scalar couplings values were taken from Ref[9].
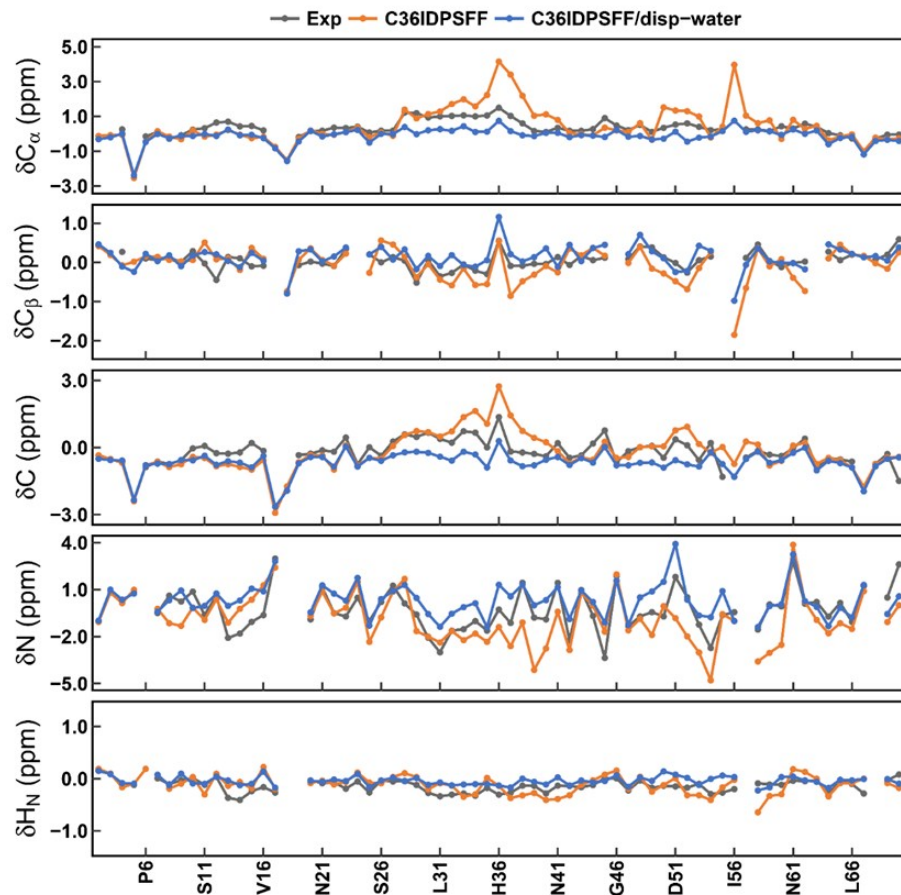
Fig. S9. Comparison of Simulated and experimental chemical shifts of Cα, Cβ, C, N, and HN atoms for ACTR. Experimental values were taken from Ref[12].
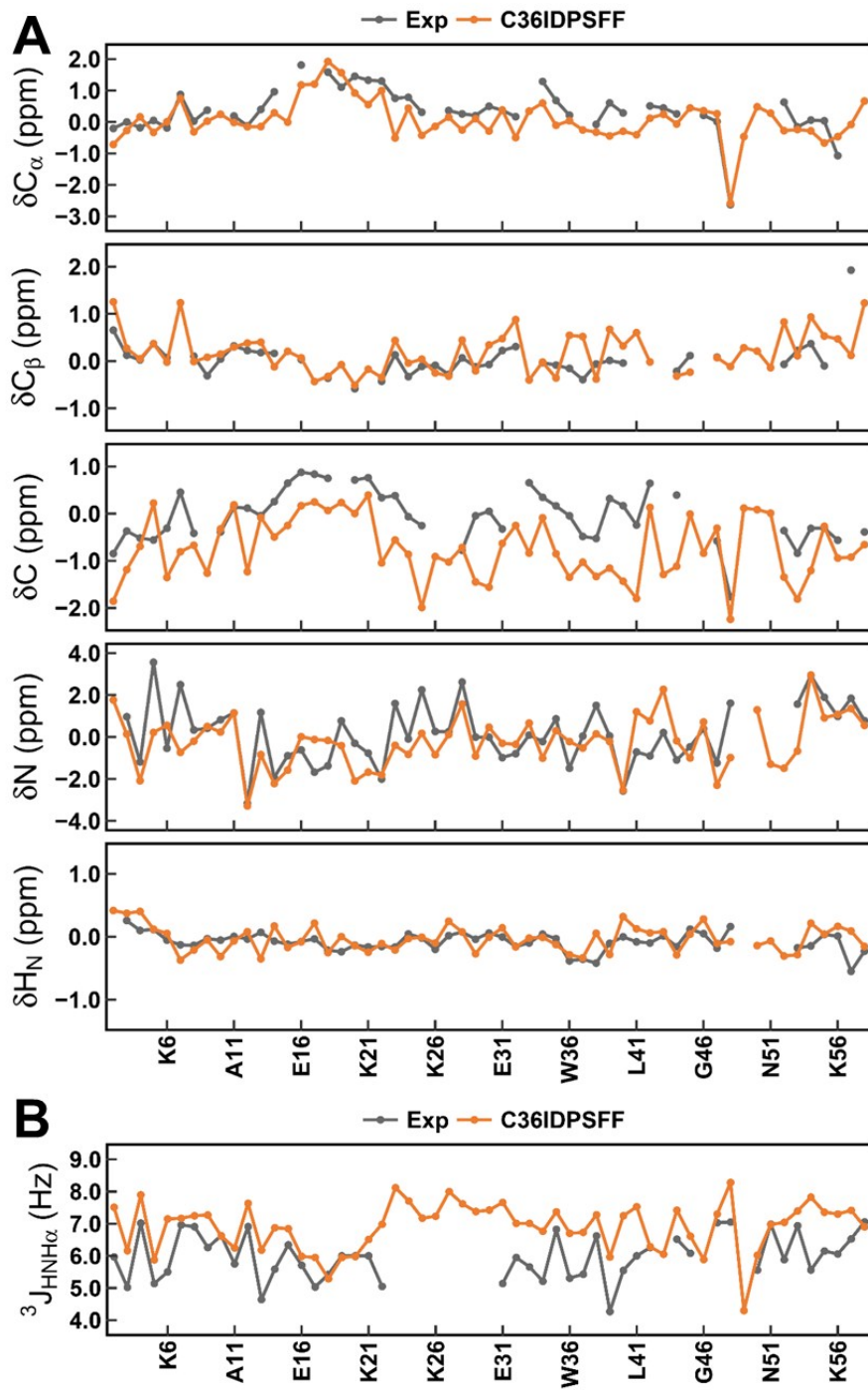
Fig. S10. Comparison of Simulated and experimental NMR observables for drkN SH3. (a) Chemical shifts of Cα, Cβ, C, N and HN atoms. (b) Backbone scalar couplings $^3J_{HNH\alpha}$. Experimental chemical shifts values were taken from Ref[13] and experimental scalar couplings values were taken from Ref[14].
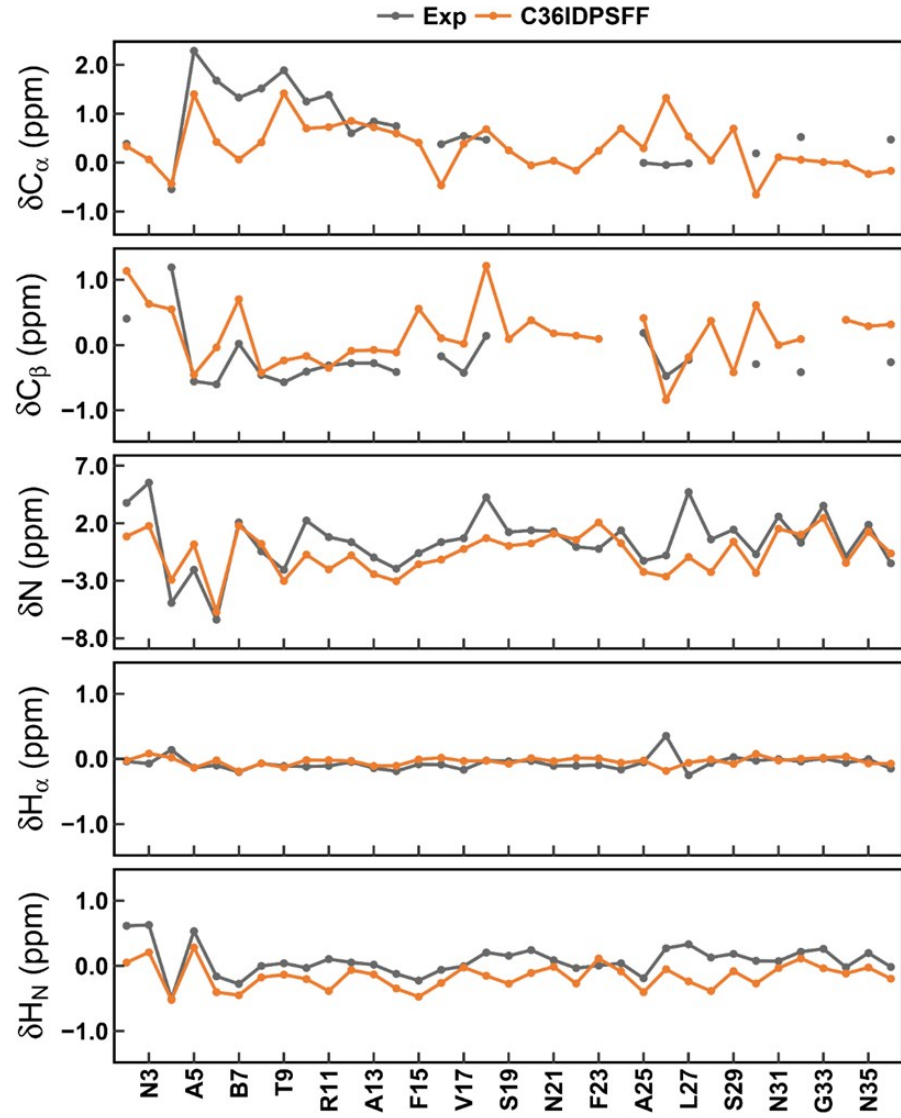
Fig. S11. Comparison of Simulated and experimental chemical shifts of Cα, Cβ, N, Hα, and HN atoms for hIAPP. Experimental values were taken from Ref[15].
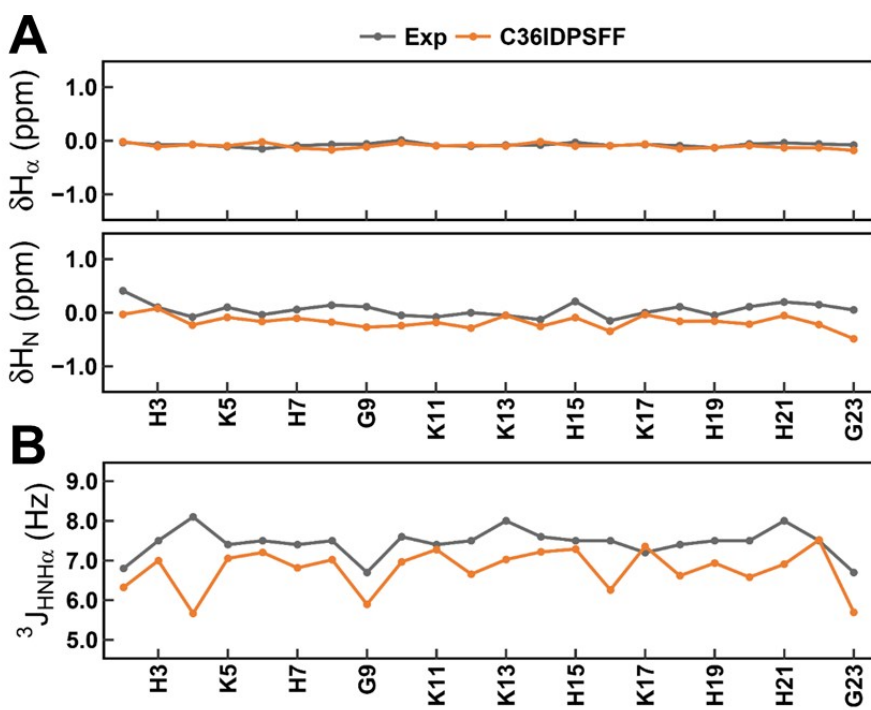
Fig. S12. Comparison of Simulated and experimental NMR observables for Histatin-5. (a) Chemical shifts of Hα and HN atoms. (b) Backbone scalar couplings $^3J_{HNH\alpha}$. Experimental values were taken from Ref[16].
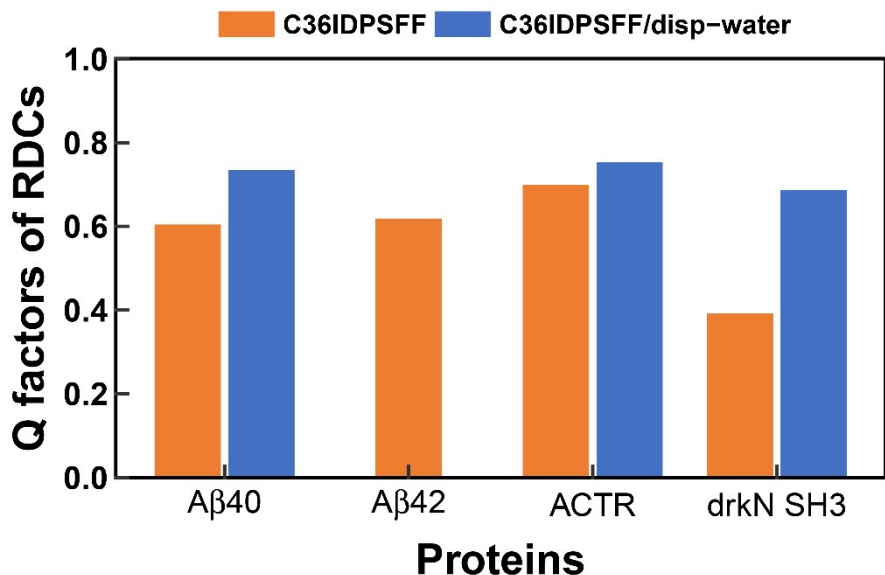
Fig. S13. Q factors of backbone N-H RDCs for disorder proteins Aβ40, Aβ42, ACTR, drkN SH3. The experimental data was taken from Ref[17-19].
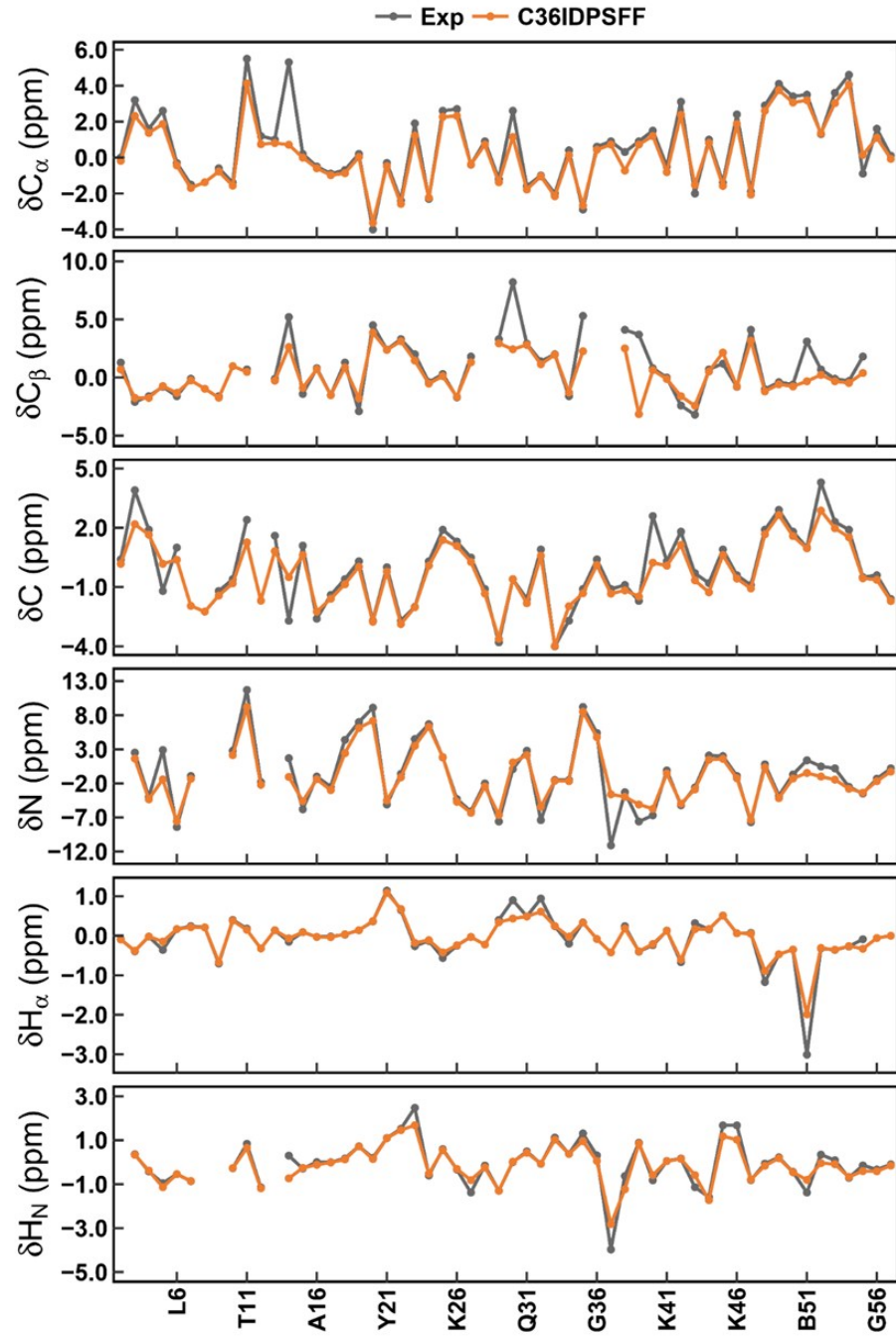
Fig. S14. Comparison of Simulated and experimental chemical shifts of Cα, Cβ, C, N, Hα and HN atoms for BPTI. Experimental values were taken from BMRB entry 5359.
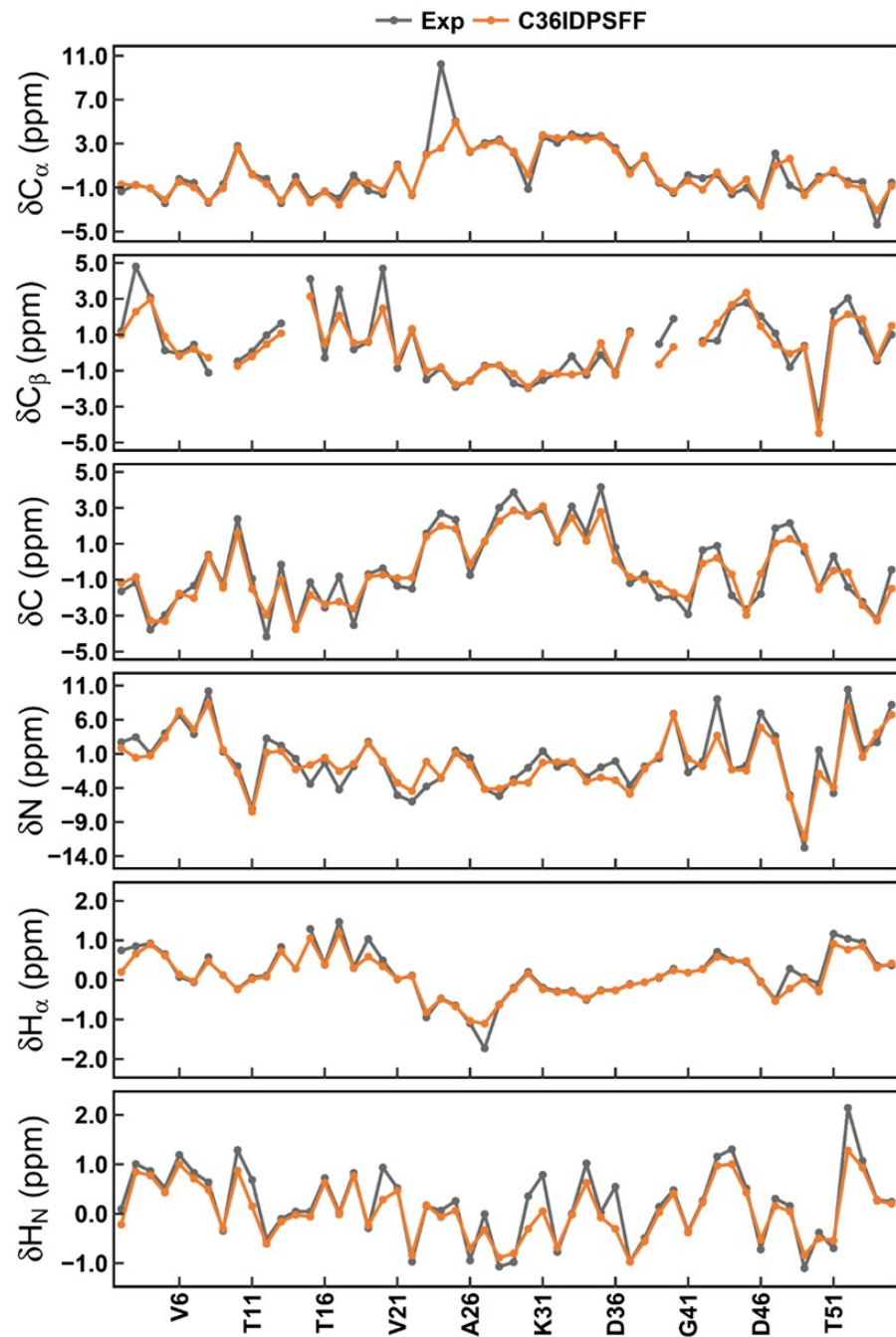
Fig. S15. Comparison of Simulated and experimental chemical shifts of Cα, Cβ, C, N, Hα and HN atoms for GB3. Experimental values were taken from Ref[20].
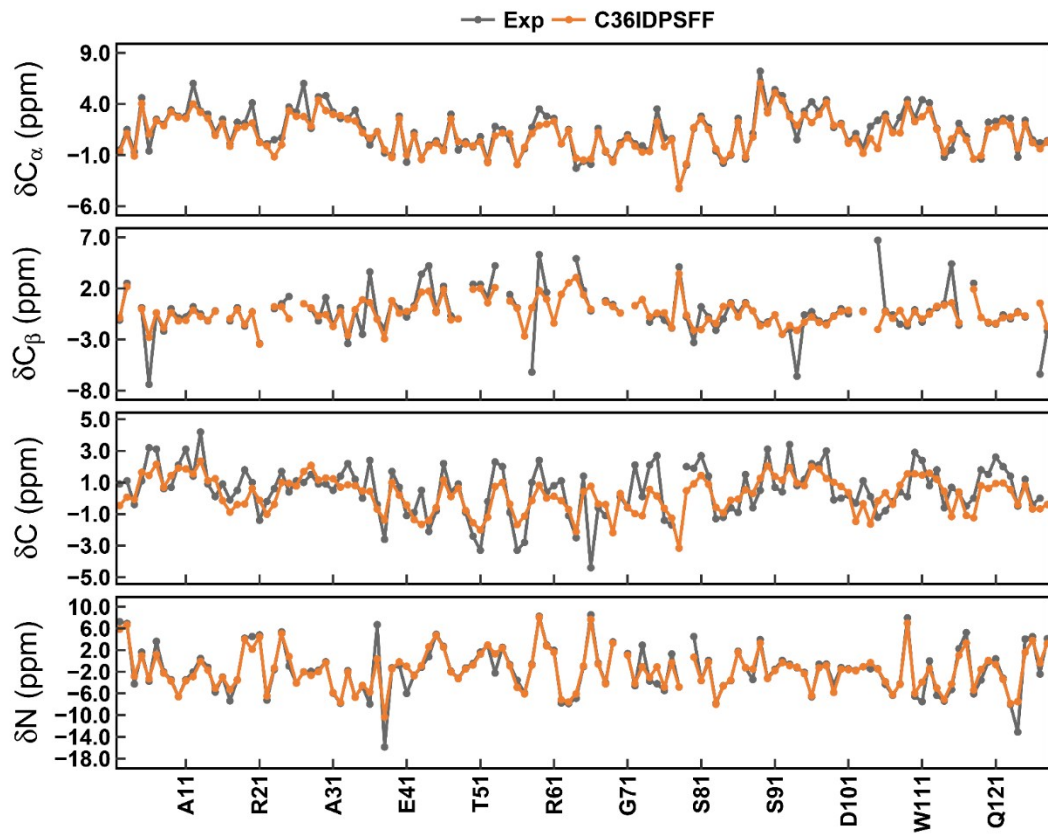
Fig. S16. Comparison of Simulated and experimental chemical shifts of Cα, Cβ, C, and N atoms for HEWL. Experimental values were taken from Ref[21].
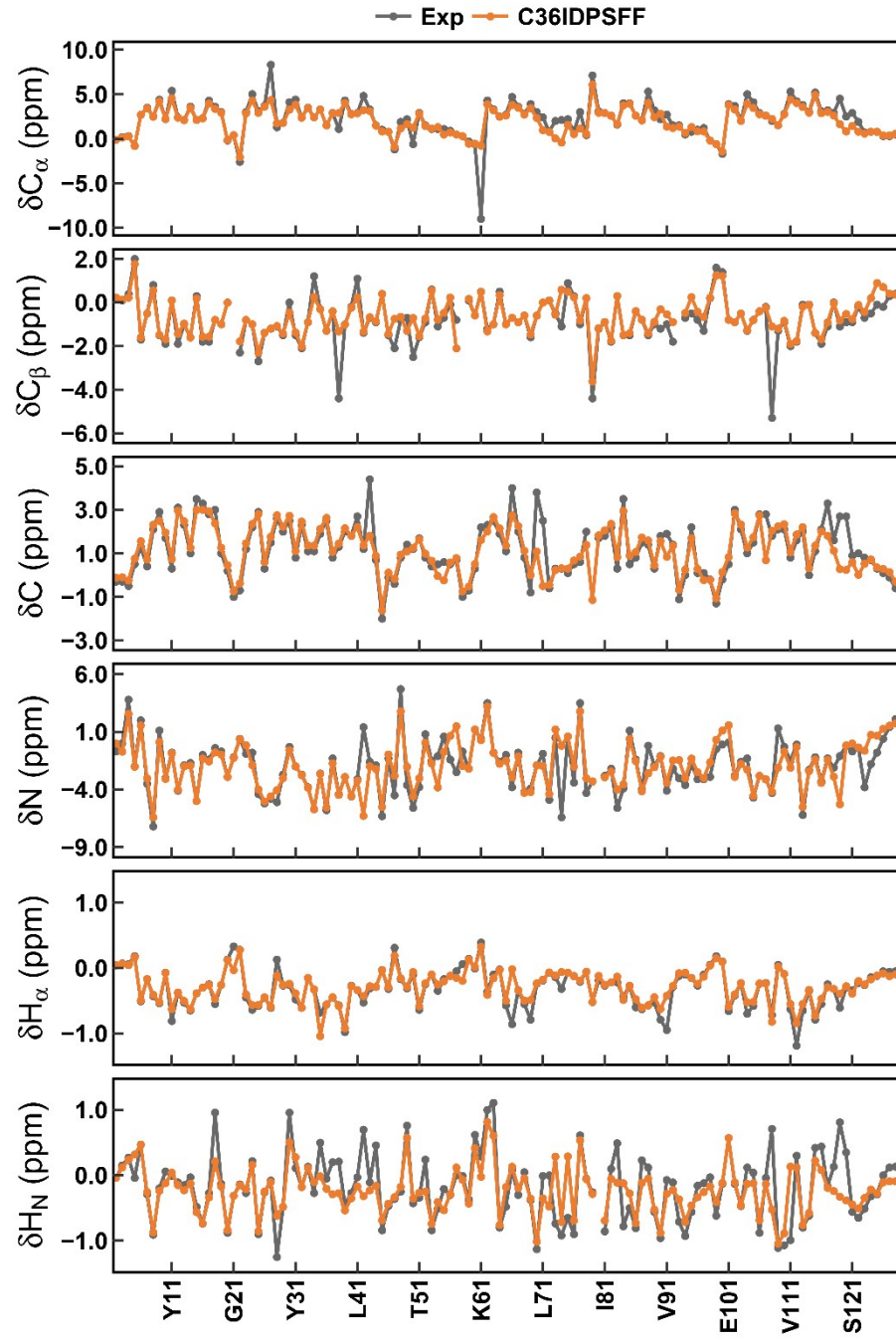
Fig. S17. Comparison of Simulated and experimental chemical shifts of Cα, Cβ, C, N, Hα, and HN atoms for 2JPU. Experimental values were taken from BMRB entry 15265.
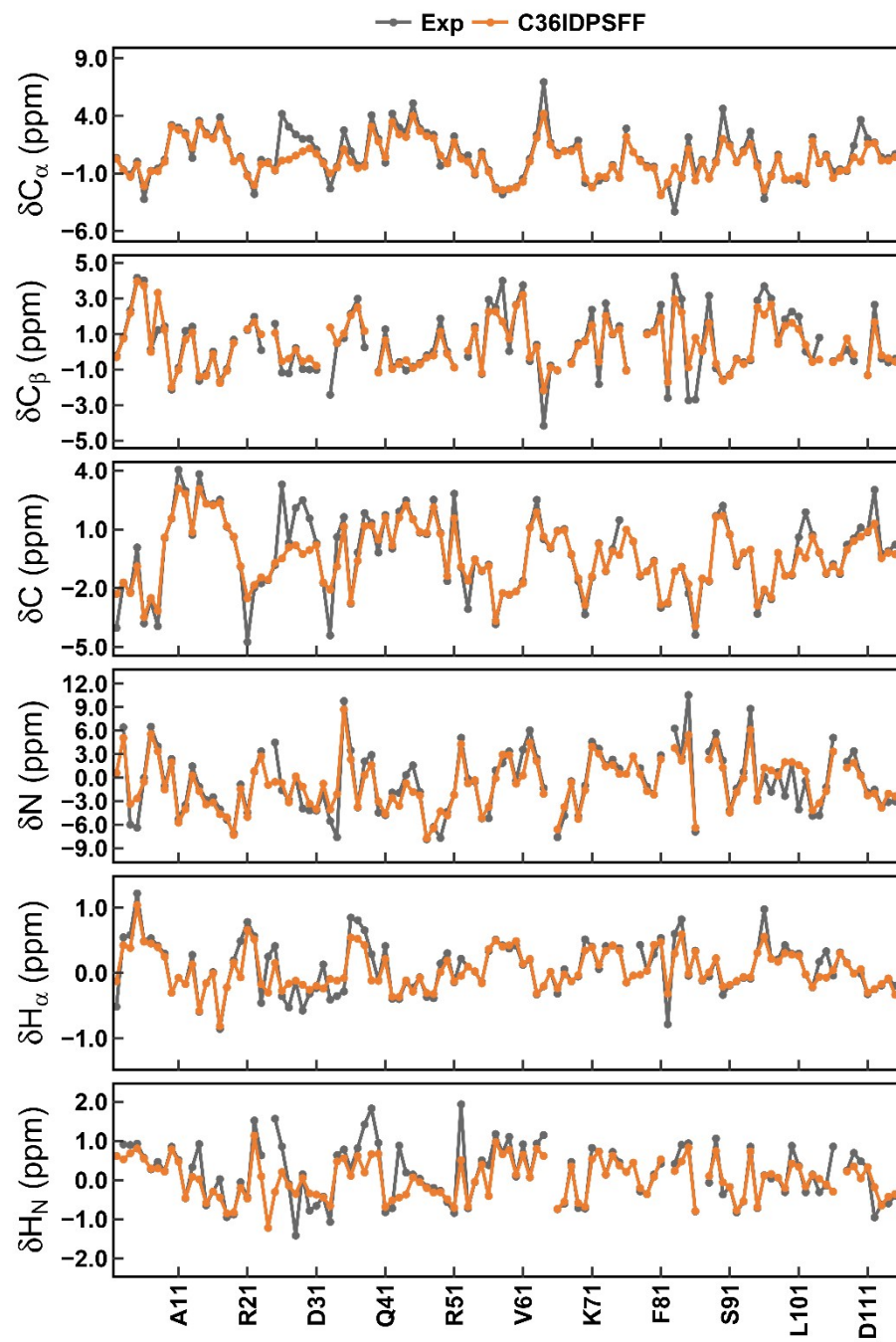
Fig. S18. Comparison of Simulated and experimental chemical shifts of Cα, Cβ, C, N, Hα, and HN atoms for 2JQN. Experimental values were taken from BMRB entry 15281.
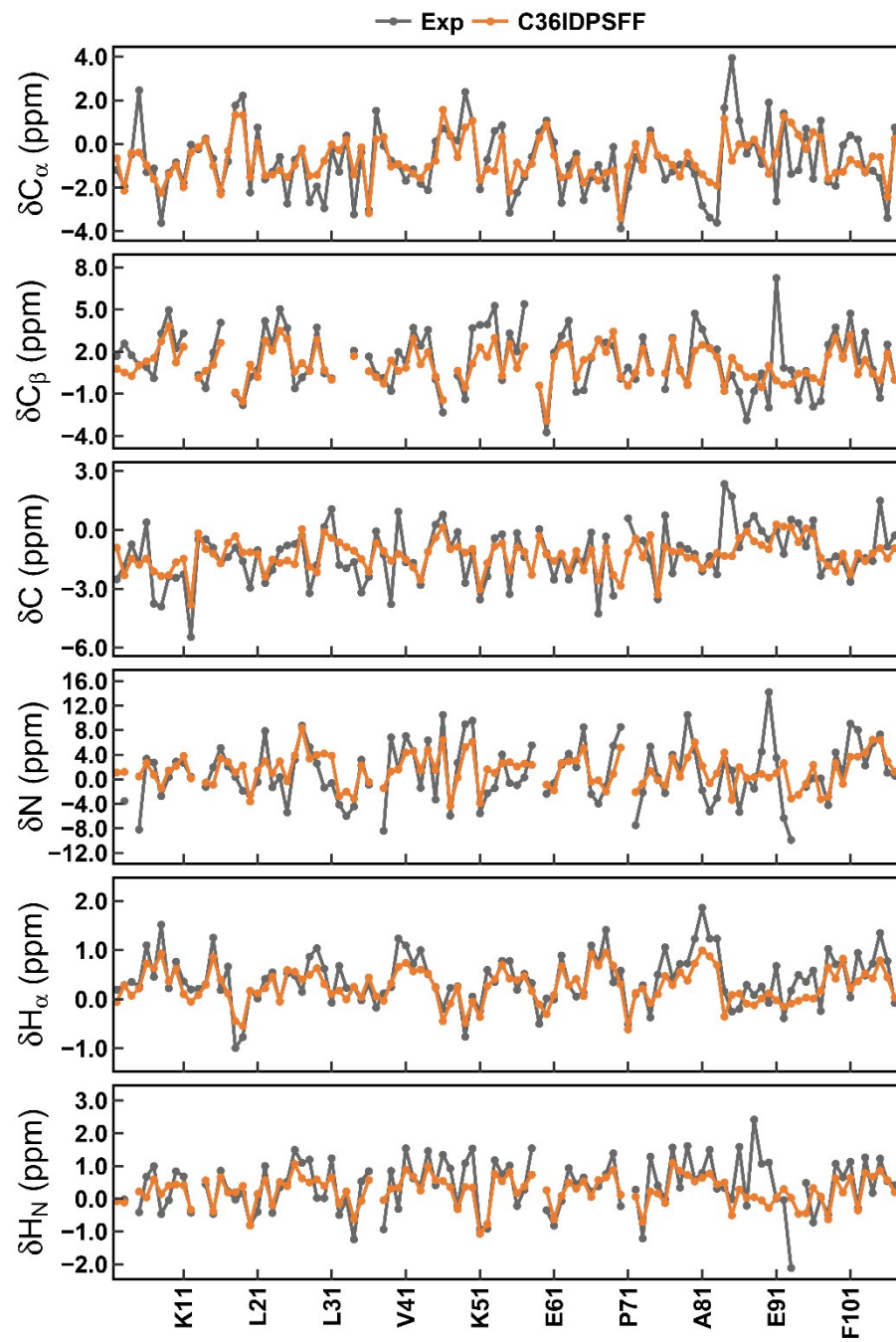
Fig. S19. Comparison of Simulated and experimental chemical shifts of Cα, Cβ, C, N, Hα, and HN atoms for 2KL6. Experimental values were taken from BMRB entry 16385.
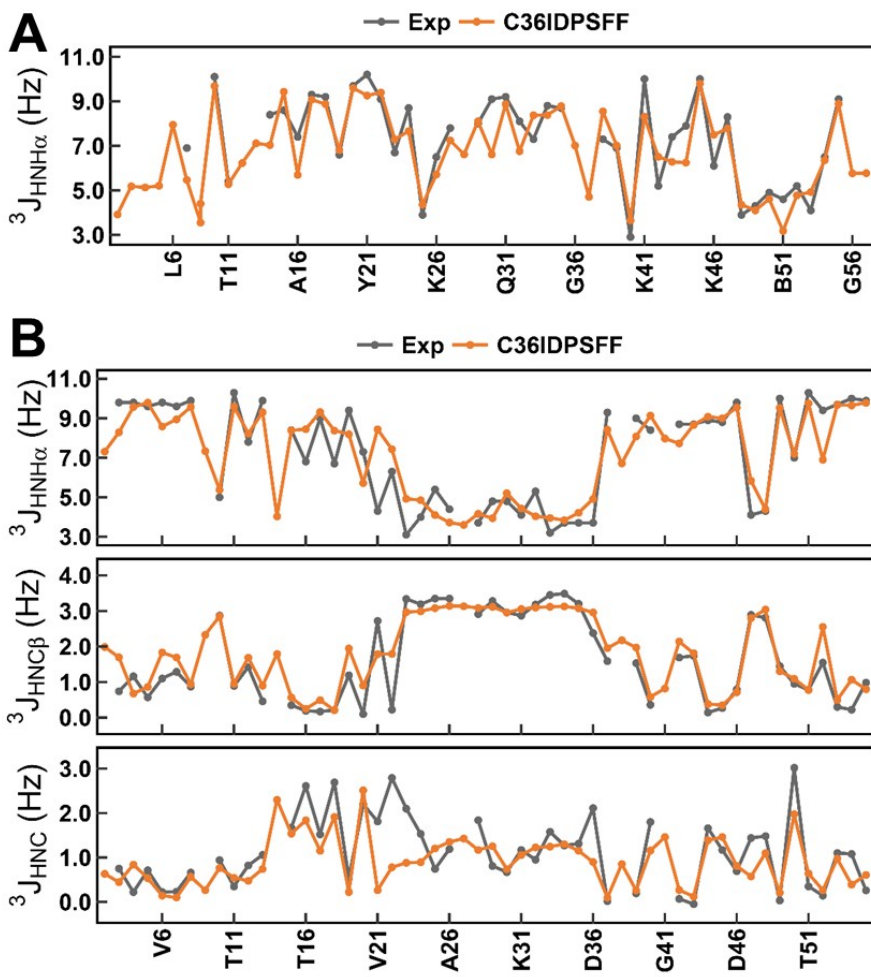
Fig. S20. Comparison of Simulated and experimental Backbone scalar couplings for folded proteins. (a) $^3J_{HNH\alpha}$ scalar couplings for BPTI. (b) $^3J_{HNH\alpha}$, $^3J_{HNC\beta}$, and $^3J_{HNC}$ scalar couplings for GB3. Experimental values were taken from Ref[1, 22].
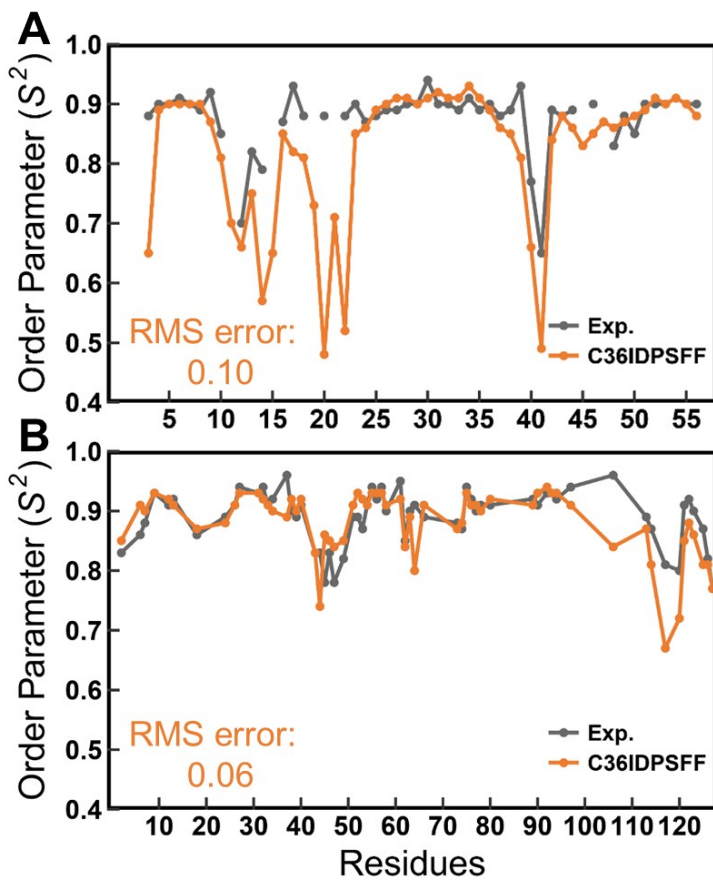
Fig. S21. Order parameter S^2 of backbone amide N-H group for folded proteins. (a) GB3. (b) HEWL. Experimental values were taken from Ref[23, 24].
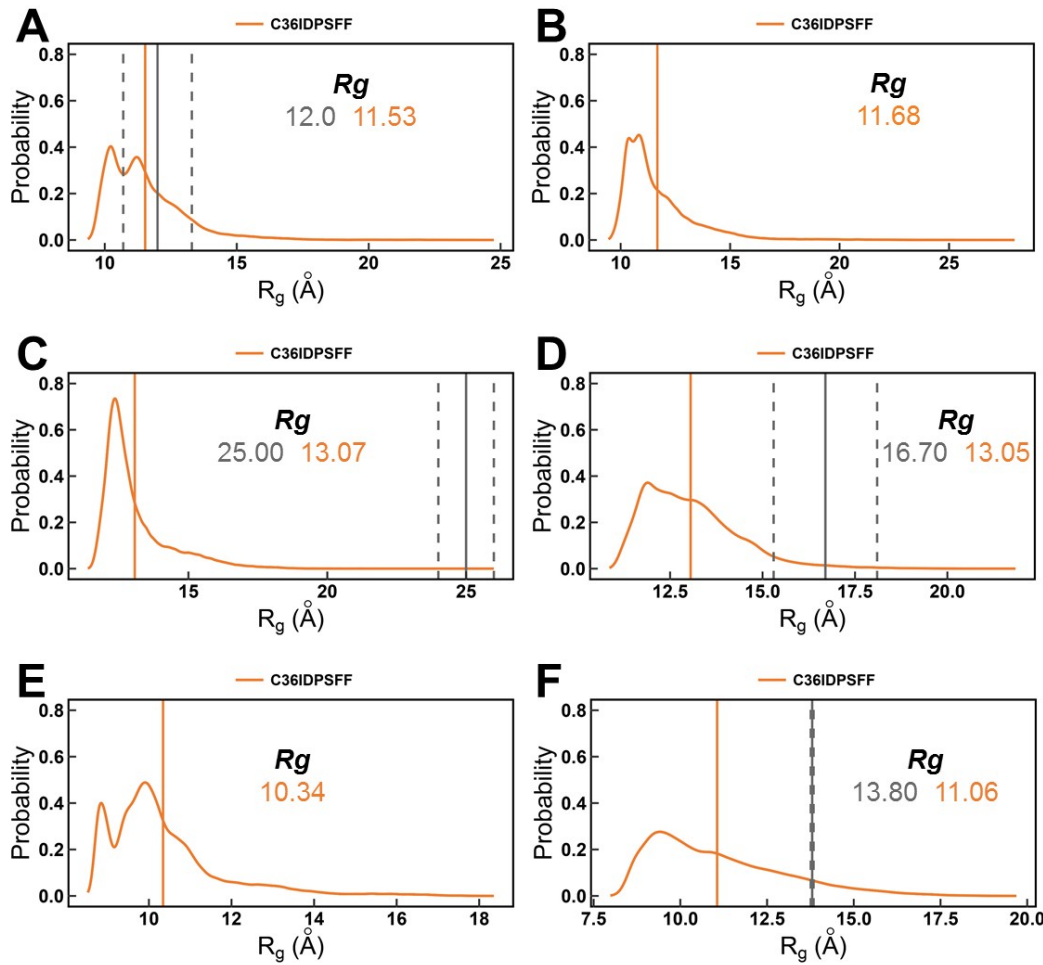
Fig. S22. Probability distributions of the simulated radii of gyration for disorder proteins. (a) Aβ40. (b) Aβ42. (c) ACTR. (d) drkN SH3. (e) hIAPP. (f) Histatin-5. The averaged *Rg* values of simulations with C36IDPSFF are marked with the vertical solid lines in orange. The experimental values[25-28] are marked with vertical solid lines in gray and the error are marked with two vertical dash lines in gray. The simulated and experimental *Rg* values are also labeled with the corresponding colors.
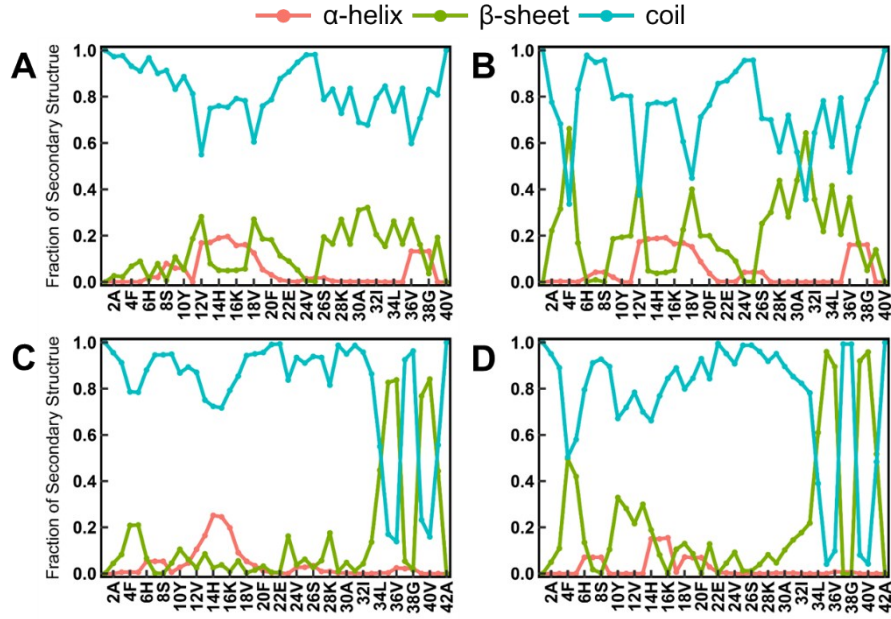
Fig. S23. The fraction of secondary structures of Aβ40 and Aβ42 in different simulation periods. (A) 200-800ns simulation of Aβ40. (B) 800-1000 ns simulation of Aβ40. (C) 200-800ns simulation of Aβ42. (D) 800-1000 ns simulation of Aβ42. The fractions of secondary structure were calculated by DSSP software. In this calculation, DSSP code "H", "G" and "I" are considered as "helix"; "B" and "E" are considered as "sheet"; "T", "S" and blanks are considered as "coil"
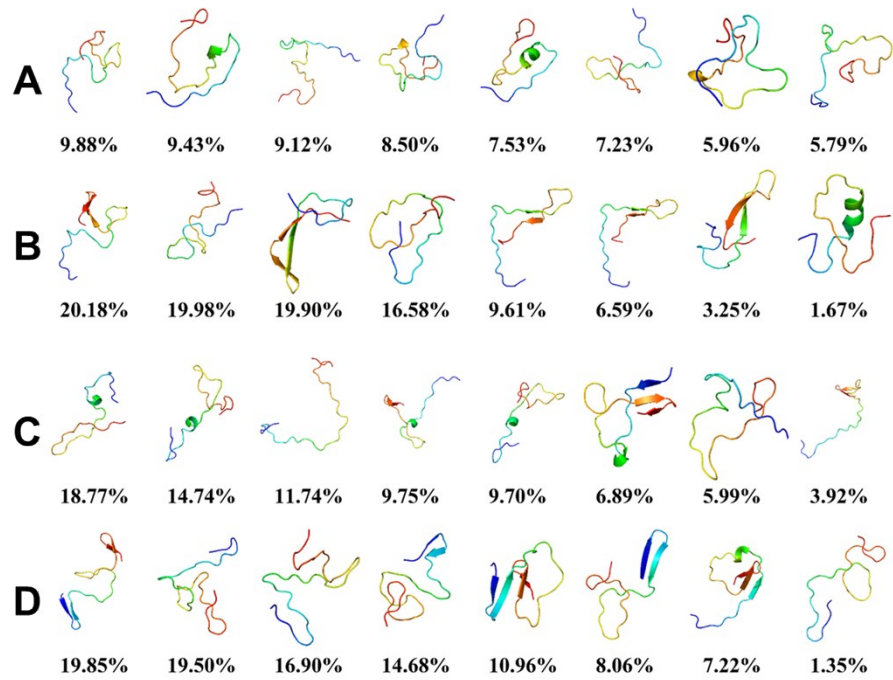
Fig. S24. Conformation clusters in the simulations of Aβ40 and Aβ40 in different simulation time. (A) Top 8 conformation clusters of Aβ40 in 200-800 ns. (B) Top 8 conformation clusters of Aβ40 in 800-1000 ns. (C) Top 8 conformation clusters of Aβ42 in 200-800 ns. (D) Top 8 conformation clusters of Aβ42 in 800-1000 ns. The percentages are labeled under the representative conformations of top clusters.
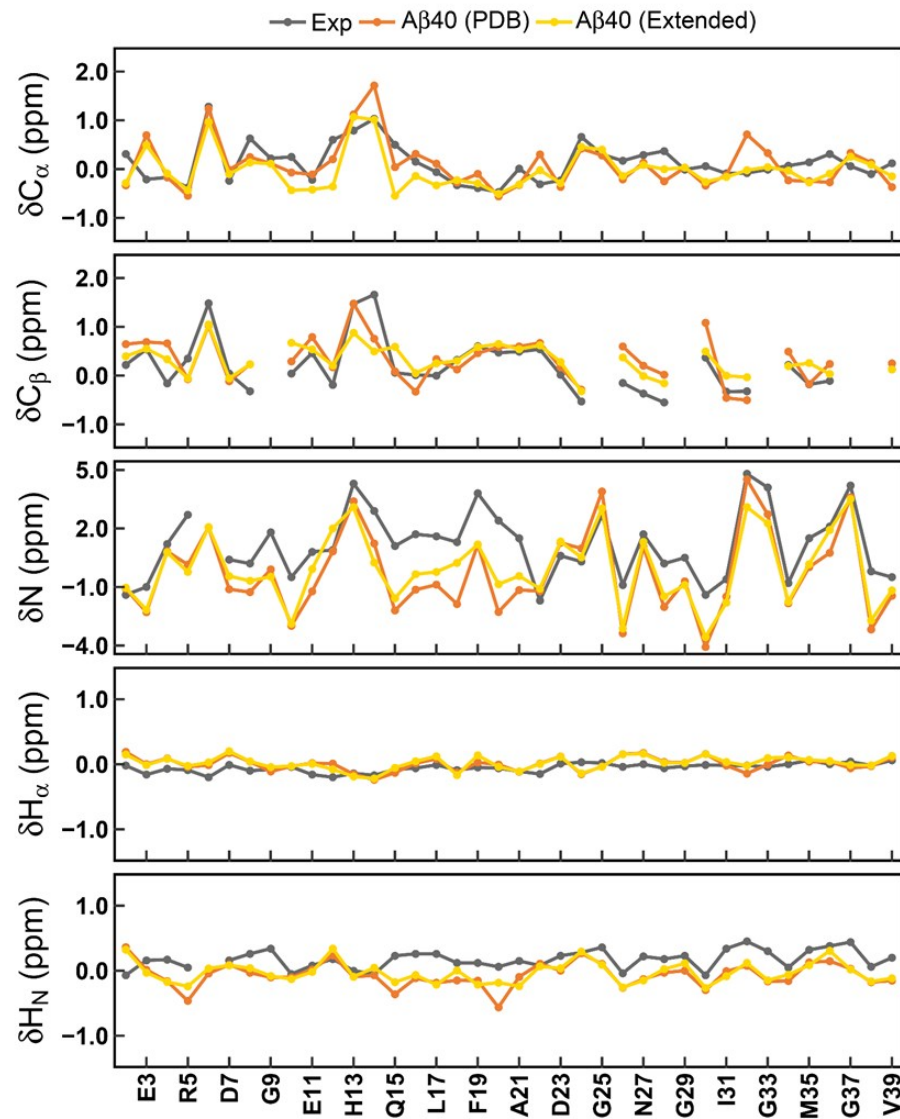
Fig. S25. Comparison of Simulated and experimental chemical shifts of Cα, Cβ, N, Hα and HN atoms for Aβ40 from two different initial structures. Experimental values are same with Figure S3
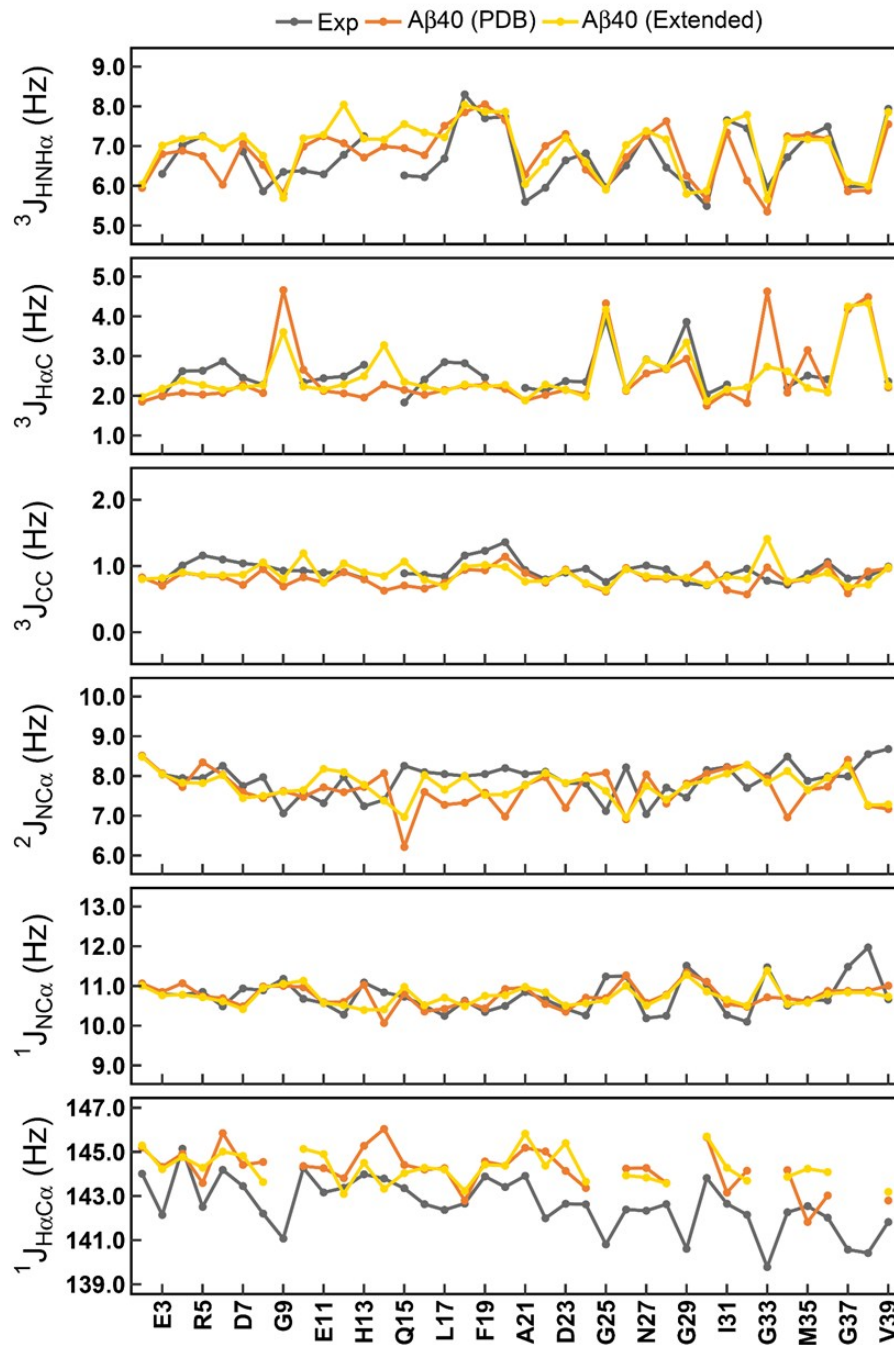
Fig. S26. Comparison of Simulated and experimental backbone scalar couplings $^3J_{HNH\alpha}$, $^3J_{H\alpha C}$, $^3J_{CC}$, $^2J_{NC\alpha}$, $^1J_{NC\alpha}$ and $^1J_{H\alpha C\alpha}$ for Aβ40 from two different initial structures. Experimental values are same with Figure S4
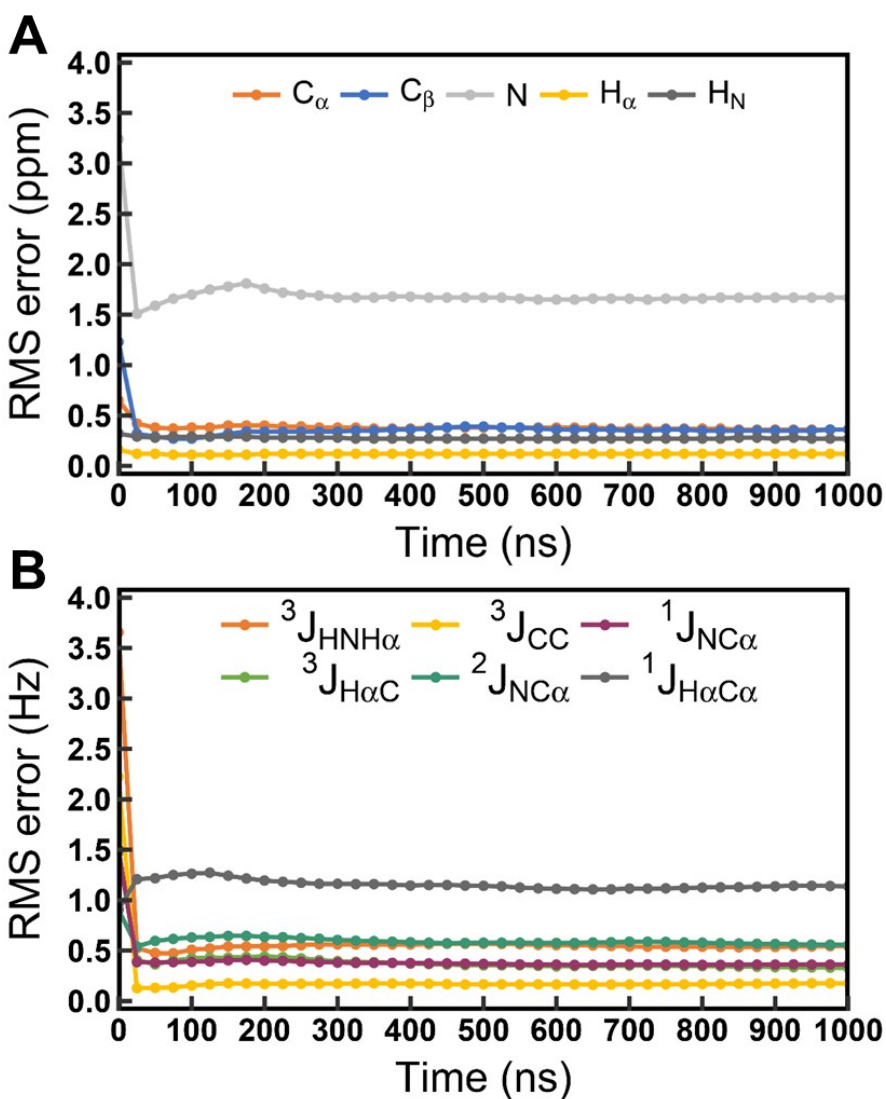
Fig. S27. Time-dependent RMS errors between experimental data and cumulative-averaged simulated chemical shifts for Aβ40 initial from an extended structure.

References

(1) Vogeli, B.; Ying, J. F.; Grishaev, A.; Bax, A., Limits on variations in protein backbone dynamics from precise measurements of scalar couplings. *J. Am. Chem. Soc.* **2007**, 129, 9377-9385.

(2) And, J. S. H.; Bax, A., Determination of φ and χ1 Angles in Proteins from 13C−13C Three-Bond J Couplings Measured by Three-Dimensional Heteronuclear NMR. How Planar Is the Peptide Bond? *J. Am. Chem. Soc.* **1997**, 119.

(3) Hennig, M.; Bermel, W.; Schwalbe, H.; Griesinger, C., Determination of psi torsion angle restraints from (3)J(C-alpha,C-alpha) and 3J(C-alpha,H-N) coupling constants in proteins. *J. Am. Chem. Soc.* **2000**, 122, 6268-6277.

(4) Lee, J. H.; Li, F.; Grishaev, A.; Bax, A., Quantitative residue-specific protein backbone torsion angle dynamics from concerted measurement of 3J couplings. *J. Am. Chem. Soc.* **2015**, 137, 1432-1435.

(5) Ding, K. Y.; Gronenborn, A. M., Protein backbone H-1(N)-C-13(alpha) and N-15-C-13(alpha) residual dipolar and J couplings: New constraints for NMR structure determination. *J. Am. Chem. Soc.* **2004**, 126, 6232-6233.

(6) Wirmer, J.; Schwalbe, H., Angular dependence of (1)J(N-i,C-alpha i) and (2)J(N-i,C alpha(i-1)) coupling constants measured in J-modulated HSQCs. *J. Biomol. NMR* **2002**, 23, 47-55.

(7) Mantsyzov, A. B.; Shen, Y.; Lee, J. H.; Hummer, G.; Bax, A., MERA: a webserver for evaluating backbone torsion angle distributions in dynamic and disordered proteins from NMR data. *J. Biomol. NMR* **2015**, 63, 85-95.

(8) Hou, L.; Shao, H.; Zhang, Y.; Li, H.; Menon, N. K.; Neuhaus, E. B.; Brewer, J. M.; Byeon, I. J.; Ray, D. G.; Vitek, M. P., Solution NMR studies of the A beta(1-40) and A beta(1-42) peptides establish that the Met35 oxidation state affects the mechanism of amyloid formation. *J. Am. Chem. Soc.* **2004**, 126, 1992-2005.

(9) Roche, J.; Shen, Y.; Lee, J. H.; Ying, J. F.; Bax, A., Monomeric A beta(1-40) and A beta(1-42) Peptides in Solution Adopt Very Similar Ramachandran Map Distributions That Closely Resemble Random Coil. *Biochemistry* **2016**, 55, 762-775.

(10) Graf, J.; Nguyen, P. H.; Stock, G.; Schwalbe, H., Structure and dynamics of the homologous series of alanine peptides: A joint molecular dynamics/NMR study. *J. Am. Chem. Soc.* **2007**, 129, 1179-1189.

(11) Walti, M. A.; Orts, J.; Vogeli, B.; Campioni, S.; Riek, R., Solution NMR studies of recombinant Abeta(1-42): from the presence of a micellar entity to residual beta-sheet structure in the soluble species. *ChemBioChem* **2015**, 16, 659-669.

(12) Ebert, M. O.; Bae, S. H.; Dyson, H. J.; Wright, P. E., NMR relaxation study of the complex formed between CBP and the activation domain of the nuclear hormone receptor coactivator ACTR. *Biochemistry* **2008**, 47, 1299-1308.

(13) Lee, J. H.; Zhang, D.; Hughes, C.; Okuno, Y.; Sekhar, A.; Cavagnero, S., Heterogeneous binding of the SH3 client protein to the DnaK molecular chaperone. *Proc. Natl. Acad. Sci. U. S. A.* **2015**, 112, E4206-4215.

(14) Zhang, O.; Forman-Kay, J. D., Structural characterization of folded and unfolded states of an SH3 domain in equilibrium in aqueous buffer. *Biochemistry* **1995**, 34, 6784-6794.

(15) Rodriguez Camargo, D. C.; Tripsianes, K.; Buday, K.; Franko, A.; Gobl, C.; Hartlmuller, C.; Sarkar, R.; Aichler, M.; Mettenleiter, G.; Schulz, M.; Boddrich, A.; Erck, C.; Martens, H.; Walch, A. K.; Madl, T.; Wanker, E. E.; Conrad, M.; de Angelis, M. H.; Reif, B., The redox environment triggers conformational changes and aggregation of hIAPP in Type II Diabetes. *Sci. Rep.* **2017**, 7, 44041.

(16) Raj, P. A.; Marcus, E.; Sukumaran, D. K., Structure of human salivary histatin 5 in aqueous and nonaqueous solutions. *Biopolymers* **1998**, 45, 51-67.

(17) Yan, Y.; McCallum, S. A.; Wang, C., M35 oxidation induces Abeta40-like structural and dynamical changes in Abeta42. *J. Am. Chem. Soc.* **2008**, 130, 5394-5395.

(18) Iesmantavicius, V.; Jensen, M. R.; Ozenne, V.; Blackledge, M.; Poulsen, F. M.; Kjaergaard, M., Modulation of the Intrinsic Helix Propensity of an Intrinsically Disordered Protein Reveals Long-Range Helix-Helix Interactions. *J. Am. Chem. Soc.* **2013**, 135, 10155-10163.

(19) Marsh, J. A.; Baker, J. M. R.; Tollinger, M.; Forman-Kay, J. D., Calculation of residual dipolar couplings from disordered state ensembles using local alignment. *J. Am. Chem. Soc.* **2008**, 130, 7804-+.

(20) Li, F.; Grishaev, A.; Ying, J.; Bax, A., Side Chain Conformational Distributions of a Small Protein Derived from Model-Free Analysis of a Large Set of Residual Dipolar Couplings. *J. Am. Chem. Soc.* **2015**, 137, 14798-14811.

(21) Schwalbe, H.; Grimshaw, S. B.; Spencer, A.; Buck, M.; Boyd, J.; Dobson, C. M.; Redfield, C.; Smith, L. J., A refined solution structure of hen lysozyme determined using residual dipolar coupling data. *Protein Sci.* **2001**, 10, 677-688.

(22) Balasubramanian, S.; Nirmala, R.; Beveridge, D. L.; Bolton, P. H., Comparison of the 13C relaxation times and proton scalar couplings of BPTI with values predicted by molecular dynamics. *J. Magn. Reson. B* **1994**, 104, 240-249.

(23) Yao, L. S.; Grishaev, A.; Cornilescu, G.; Bax, A., Site-Specific Backbone Amide N-15 Chemical Shift Anisotropy Tensors in a Small Protein from Liquid Crystal and Cross-Correlated Relaxation Measurements. *J. Am. Chem. Soc.* **2010**, 132, 4295-4309.

(24) Buck, M.; Boyd, J.; Redfield, C.; MacKenzie, D. A.; Jeenes, D. J.; Archer, D. B.; Dobson, C. M., Structural Determinants of Protein Dynamics: Analysis of 15N NMR Relaxation Measurements for Main-Chain and Side-

Chain Nuclei of Hen Egg White Lysozyme. *Biochemistry* **1995**, 34, 4041-4055.

(25) Granata, D.; Baftizadeh, F.; Habchi, J.; Galvagnion, C.; De Simone, A.; Camilloni, C.; Laio, A.; Vendruscolo, M., The inverted free energy landscape of an intrinsically disordered peptide by simulations and experiments. *Sci. Rep.* **2015**, 5, 15449.

(26) Gely, S.; Lowry, D. F.; Bernard, C.; Jensen, M. R.; Blackledge, M.; Costanzo, S.; Bourhis, J. M.; Darbon, H.; Daughdrill, G.; Longhi, S., Solution structure of the C-terminal X domain of the measles virus phosphoprotein and interaction with the intrinsically disordered C-terminal domain of the nucleoprotein. *J. Mol. Recognit.* **2010**, 23, 435-447.

(27) Choy, W. Y.; Mulder, F. A. A.; Crowhurst, K. A.; Muhandiram, D. R.; Millett, I. S.; Doniach, S.; Forman-Kay, J. D.; Kay, L. E., Distribution of molecular size within an unfolded state ensemble using small-angle X-ray scattering and pulse field gradient NMR techniques. *J. Mol. Biol.* **2002**, 316, 101-112.

(28) Cragnell, C.; Durand, D.; Cabane, B.; Skepo, M., Coarse-grained modeling of the intrinsically disordered protein Histatin 5 in solution: Monte Carlo simulations in combination with SAXS. *Proteins-Structure Function and Bioinformatics* **2016**, 84, 777-791.